

AD-A087 033

ROCKWELL INTERNATIONAL ANAHEIM CA ELECTRONIC DEVICES DIV F/6 7/4

GAAS SURFACE EFFECTS.(U)

MAR 80 G KINOSHITA, G G KUHLMANN

F33615-78-C-1591

UNCLASSIFIED

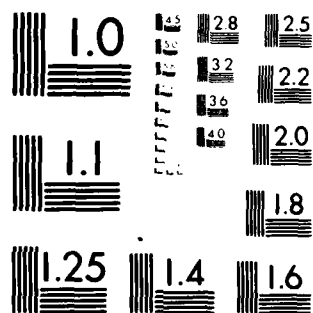
C79-1032/501

AFWAL-TR-80-1018

NL

1-1  
AL  
20-1-83

END  
DATE  
FILMED  
9-80  
DTIC



MICROCOPY RESOLUTION TEST CHART  
NATIONAL BUREAU OF STANDARDS-1963-A

ADA 087033

18  
19  
AFWAL TR-80-1018

LEVEL

A075 478



6  
GaAs SURFACE EFFECTS,

ROCKWELL INTERNATIONAL  
ELECTRONIC DEVICES DIVISION  
3370 MIRALOMA AVENUE  
P.O. BOX 4761  
ANAHEIM, CALIFORNIA 92803

DTIC  
ELECTE  
JUL 27 1980  
D  
C

11  
MAR 1980

12 61

10 G. Kinoshita Gordon G. Kuhlmann  
TECHNICAL REPORT AFWAL-TR-80-1018

9 Interim Technical 1 Jul 1978 1 Jul 1979,

15 F33615-78-C-1591

16  
23p5

Approved for public release; distribution unlimited.

17 R1

14 C77-1032/501

AVIONICS LABORATORY  
AIR FORCE WRIGHT AERONAUTICAL LABORATORIES  
AIR FORCE SYSTEMS COMMAND  
WRIGHT-PATTERSON AIR FORCE BASE, OHIO 45433

DDC FILE COPY

410 530  
80 7 17 017

# NOTICE

When Government drawings, specifications, or other data are used for any purpose other than in connection with a definitely related Government procurement operation, the United States Government thereby incurs no responsibility nor any obligation whatsoever; and the fact that the government may have formulated, furnished, or in any way supplied the said drawings, specifications, or other data, is not to be regarded by implication or otherwise as in any manner licensing the holder or any other person or corporation, or conveying any rights or permission to manufacture use, or sell any patented invention that may in any way be related thereto.

This report has been reviewed by the Office of Public Affairs (ASD/PA) and is releasable to the National Technical Information Service (NTIS). At NTIS, it will be available to the general public, including foreign nations.

This technical report has been reviewed and is approved for publication.



ROBERT L. JOHNSON, Capt, USAF  
Project Engineer

FOR THE COMMANDER



PHILIP E. STOVER, Chief  
Electronic Research Branch  
Avionics Laboratory

"If your address has changed, if you wish to be removed from our mailing list, or if the addressee is no longer employed by your organization please notify AFWAL/AADR, W-PAFB, OH 45433 to help us maintain a current mailing list".

Copies of this report should not be returned unless return is required by security considerations, contractual obligations, or notice on a specific document.

REPORT DOCUMENTATION PAGE		READ INSTRUCTIONS BEFORE COMPLETING FORM
1. REPORT NUMBER AFWAL-TR-1018	2. GOVT ACCESSION NO. AD A087033	3. RECIPIENT'S CATALOG NUMBER
4. TITLE (and Subtitle) GaAs Surface Effects	5. TYPE OF REPORT & PERIOD COVERED Interim Technical July 1, 1978-July 1, 1979	
7. AUTHOR(s) G. Kinoshita Gordon G. Kuhlmann	6. PERFORMING ORG. REPORT NUMBER C79-1032/501 ✓	
9. PERFORMING ORGANIZATION NAME AND ADDRESS Rockwell International Corporation ✓ Electronics Research Center 3370 Miraloma Ave., Anaheim, CA 92803	8. CONTRACT OR GRANT NUMBER(s) F33615-78-C-1591 ✓	
11. CONTROLLING OFFICE NAME AND ADDRESS	10. PROGRAM ELEMENT, PROJECT, TASK AREA & WORK UNIT NUMBERS 61102F 2305-R1-82	
14. MONITORING AGENCY NAME & ADDRESS (if different from Controlling Office) Avionics Laboratory (AFWAL/AADR) AF Wright Aeronautical Laboratories (AFSC) Wright-Patterson Air Force Base, Ohio 45433	12. REPORT DATE March 1980	
	13. NUMBER OF PAGES 59	
	15. SECURITY CLASS. (of this report) Unclassified.	
16. DISTRIBUTION STATEMENT (of this Report)  Approved for public release; distribution unlimited.		
17. DISTRIBUTION STATEMENT (of the abstract entered in Block 20, if different from Report)  Same as block 16.		
18. SUPPLEMENTARY NOTES		
19. KEY WORDS (Continue on reverse side if necessary and identify by block number) Gallium Arsenide                      Ion Microprobe Analysis Oxidation                              Gallium Arsenide Phosphide Ion Implantation                      Phosphorus Ions Annealing                               Insulator		
20. ABSTRACT (Continue on reverse side if necessary and identify by block number) This report presents the results of the first six months of a program to investigate the passivation of GaAs surfaces using a native insulator. Ion implantation of phosphorus and subsequent oxidation of the surface was used to form the insulator. Post-implant annealing indicates that CVD SiO <sub>2</sub> has somewhat better encapsulating properties than sputtered Si <sub>3</sub> N <sub>4</sub> . It was found that high-dose phosphorus implantation significantly reduces decomposition of the semiconductor surface under the SiO <sub>2</sub> encapsulant during high-temperature annealing. → ne ✓		

Annealed and unannealed surfaces were oxidized at 600°C in dry O<sub>2</sub>. Results of the oxidations demonstrated that the highest quality films are grown on unannealed surfaces which received doses of 1 to 2 x 10<sup>16</sup> phosphorus ions/cm<sup>2</sup> implanted at energies of 30 to 60 keV.

The C-V characteristics of oxides grown at 600°C in dry O<sub>2</sub> over phosphorus implanted GaAs exhibit characteristics resembling those grown on bulk GaAs<sub>1-x</sub>P<sub>x</sub>, including hysteresis and deep depletion. The conductivity of the oxides formed over implanted material is about an order of magnitude higher than that on bulk material.

Ion microprobe analysis of the implant profiles indicate that phosphorus diffusion is not significant during either high-temperature annealing or oxidation. Elemental depth profiles of oxide layers indicate phosphorus incorporation into the film in the region from the peak of the implant to the interface with the semiconductor. A lack of arsenic and phosphorus at the oxide surfaces indicates that this region may be composed primarily of Ga<sub>2</sub>O<sub>3</sub>.

Accession For	
NTIS GRA&I	<input checked="checked" type="checkbox"/>
DDC TAB	<input type="checkbox"/>
Unannounced	<input type="checkbox"/>
Justification	
By	
Distribution/	
Availability	
Dist	Availability special
A	

Unclassified

## FOREWORD

This report presents the results of the first year of a program to investigate the passivation of GaAs surfaces using a native insulator. Ion implantation of phosphorus and subsequent oxidation of the surface was used to form the insulator. Ion implantation, annealing and oxidation experiments were conducted to define the conditions necessary for thermal oxide growth on GaAs substrates.

Post-implant annealing indicates that CVD  $\text{SiO}_2$  has somewhat better encapsulating properties than sputtered or plasma  $\text{Si}_3\text{N}_4$  for experimental conditions employed in this program. High-dose phosphorus implantation was shown to significantly reduce decomposition of the semiconductor surface under the  $\text{SiO}_2$  encapsulant during high-temperature annealing.

Annealed and unannealed surfaces were oxidized at  $600^\circ\text{C}$  in dry  $\text{O}_2$ . Results of the oxidations demonstrated that the highest quality films were grown on unannealed surfaces which received doses of  $1$  to  $2 \times 10^{16}$  phosphorus ions/ $\text{cm}^2$  implanted at energies of  $30$  to  $60$  KeV.

The C-V characteristics of oxides grown at  $600^\circ\text{C}$  in dry  $\text{O}_2$  over phosphorus implanted GaAs exhibit characteristics resembling those grown on bulk  $\text{GaAs}_{1-x}\text{P}_x$ , including hysteresis and deep depletion. The conductivity of the oxides formed over implanted material is about an order of magnitude higher than that on bulk material.

Ion microprobe analysis of the implant profiles indicate that phosphorus diffusion is not significant during high-temperature annealing or oxidation. Elemental depth profiles of oxide layers indicate phosphorus incorporation into

the film in the region from the peak of the implant to the interface with the semiconductor. A lack of arsenic and phosphorus at the oxide surface indicates that this region may be composed primarily of  $\text{Ga}_2\text{O}_3$ .

This report is the second interim technical report generated under AFWAL Contract F33615-78-C-1591. The first interim technical report was issued under Report No. AFAL-TR-79-1058 (same title).



## Table of Contents

	<u>Page</u>
I. INTRODUCTION . . . . .	1
II. NATIVE SURFACE PASSIVATION LAYER FORMATION ON GaAs USING ION-IMPLANTATION AND SUBSEQUENT OXIDATION . . . . .	4
Basic Approach . . . . .	4
Synthesis of $\text{GaAs}_{1-x}\text{P}_x$ and $\text{Ga}_{1-x}\text{Al}_x$ by Ion-Implantation into GaAs . . . . .	6
Phosphorus Implantation Dose and Energy Considerations . . . . .	7
Additional Considerations in Forming $\text{GaAs}_{1-x}\text{P}_x$ Layers . . . . .	12
Phosphorus Implant Damage . . . . .	12
Post-Implant Encapsulation and Annealing . . . . .	14
Oxidation Considerations . . . . .	15
Oxidation Temperature and Time . . . . .	15
Oxide Thickness . . . . .	15
Redistribution of Implanted Phosphorus . . . . .	16
III. RESULTS OF ION IMPLANTATION, ANNEALING AND OXIDATION EXPERIMENTS . . . . .	17
Starting Material and Surface Preparation . . . . .	17
GaAs Starting Material . . . . .	17
Substrate Surface Preparation . . . . .	17
Ion Implantation . . . . .	18
Encapsulation and Annealing Experiments . . . . .	19
Silicon Nitride . . . . .	19

Room Temperature Implantation and Annealing Variations Using SiO <sub>2</sub> /Native Oxide Encapsulants . . . . .	21
High-Temperature Implantation Using SiO <sub>2</sub> Encapsulant . . . . .	23
Oxidation Experiments - Phosphorus Implanted GaAs . . . . .	24
Oxidation of SiO <sub>2</sub> -Encapsulated and Annealed Surfaces . . . . .	26
Annealing Temperature Effects . . . . .	26
Implant Dose Effects . . . . .	26
Hot Implants . . . . .	28
Implant Energy Effects . . . . .	28
Oxidation of Unannealed Implanted Surfaces . . . . .	30
Implant Dose Effects . . . . .	30
Implant Energy Effects . . . . .	31
Hot Implants . . . . .	33
Aluminum Implanted GaAs . . . . .	34
MIS Capacitor Experiments . . . . .	36
Ion Microprobe Analysis of Implant Profiles and Oxide Composition . . . . .	41
IV. SUMMARY AND CONCLUSIONS . . . . .	47
Ion Implantation and Annealing . . . . .	47
Oxidation . . . . .	48
CONCLUSIONS . . . . .	49
REFERENCES . . . . .	50

## List of Illustrations

<u>Figure</u>		<u>Page</u>
1	Process Steps Used to Form a Thermal Oxide Using Phosphorus Ion-Implantation . . . . .	5, 6
2	Phosphorus Implant Profile . . . . .	9
3	Boundary Between Implanted and Unimplanted Region Following Anneal at 725°C Using SiO <sub>2</sub> Encapsulant (247X) . . . . .	23
4	Photomicrograph of Oxide Surface (247X), (a) Regions of GaAs Implanted with $1.8 \times 10^{16}$ $\text{cm}^{-2}$ <sup>31</sup> P+ at 190 keV and Annealed with Silox Encapsulant at 725°C, N <sub>2</sub> , 1 Hr.; (b) Unimplanted Region Same Wafer . . . . .	25
5	Surface Following Annealing at 650°C in N <sub>2</sub> , 1 Hr. and Oxidation at 600°C, 30 min., (SiO <sub>2</sub> Encapsulant (97X) . . . . .	27
6	Nomarski Photomicrograph of Oxide Grown on Annealed Implanted Surface (Dose: $3 \times 10^{16}$ $\text{cm}^{-2}$ ) (280X) . . . . .	29
7	Oxide Grown on Surface Implanted at 400°C (SiO <sub>2</sub> Encapsulant) (247X) . . . . .	29
8	Oxide Growth on Unannealed Surface Implanted at 150 keV ( $1 \times 10^{16}$ $\text{cm}^{-2}$ ) (247X) . . . . .	32
9	Oxide Growth on Unannealed Surface Implanted at 30 keV ( $1 \times 10^{16}$ $\text{cm}^{-2}$ ) (481X). (Boundary Between Uniform Oxide and Decomposed Strip Around Wafer Edge.) . . . . .	33
10	Nomarski Photomicrograph of Damage Following Oxidation of Aluminum Implanted Surface ( $5 \times 10^{16}$ $\text{cm}^{-2}$ , 50 keV) with Dry O <sub>2</sub> for 2 Hours at 600°C (151X) . . . . .	35
11	Nomarski Photomicrograph of Boundary between Implanted and Unimplanted Regions Following 650°C, N <sub>2</sub> anneal with SiO <sub>2</sub> Encapsulant (151X) . . . . .	35
12	C-V Characteristics of Oxide Grown on Ion-Implanted GaAs . . . . .	37

<u>Figure</u>		<u>Page</u>
13	C-V Characteristics of Oxide Grown on Non-Implanted GaAs . . . . .	38
14	DC Current-Voltage Characteristics of Thermal Oxides on GaAs . . . . .	40
15	IMMA Profiles of Unannealed (a) and Annealed (b) Implanted Layers . . . . .	42
16	IMMA Profile of Sample Implanted at 300°C Substrate Temperature . . . . .	44
17	IMMA Profiles of Annealed (a) and Annealed/ Oxidized (b) Implanted Layers . . . . .	45
18	IMMA Profiles of Oxides Grown on Unimplanted (a) and Unannealed Implanted (b,c) Layers . . . . .	46

## SECTION I

### INTRODUCTION

This report describes work performed from July 1, 1978 to July 1, 1979 on AFSC Contract No. F33615-78-C-1591, "GaAs Surface Effects." AFAL-TR-79-1058, whose contents are included in this report, described work on the first six months of this contract. The primary objective of this three-year research program is to investigate the passivation of gallium arsenide (GaAs) surfaces and the application of dielectric thin film overlayers in metal-insulator-semiconductor field-effect transistors (MISFETs).

Surface passivation insulators are used as barriers to deleterious environmental influences to improve the stability and performance of semiconductor devices. Thermally grown  $\text{SiO}_2$  has resulted in the highest quality passivation layers in the silicon technology; however, limited research has been performed to study the effectiveness of thermally grown native insulators as passivation layers for III-V compound semiconductors. Although many device applications require an extremely low dielectric/semiconductor interface state density, all semiconductor devices benefit from surface passivation insulators which act as a barrier to contamination and which decrease junction leakage currents.

Several different methods have been investigated for forming passivation dielectrics on GaAs. These include thermal oxidation, deposited insulators, and both liquid and plasma anodization. Most of these insulators have proved to be inadequate for many device applications because of excessive dielectric leakage, large interface state densities, and/or charge trapping in the oxide.

Oxides grown using the anodic and plasma techniques generally require post-oxidation annealing treatments at elevated temperatures for stabilization. The major difficulty associated with thermal oxidation is related to the high

equilibrium vapor pressure of arsenic above about 450°C, which results in arsenic loss and non-stoichiometry at the oxide-semiconductor interface. Because of this loss, thermal oxidation of GaAs results primarily in crystalline gallium oxide ( $\beta\text{-Ga}_2\text{O}_3$ ), which has not proven to have suitable dielectric and passivation characteristics.

Previous studies of the thermal oxidation of the alloy gallium arsenide phosphide ( $\text{GaAs}_{1-x}\text{P}_x$ ) (References 1-5) have indicated the possible importance of phosphorus, through the presence of stable gallium phosphate ( $\text{GaPO}_4$ ), in forming a higher quality dielectric than is attainable by simply oxidizing GaAs.  $\text{GaAs}_{1-x}\text{P}_x$ , unfortunately, is not the optimum choice for many of the device applications suited for GaAs. This situation occurs because the bandgap energy increases and electron mobility decreases as the phosphorus mole fraction,  $x$ , increases. If, however, only the semiconductor surface region is modified by a suitable species such as phosphorus, and later oxidized, a native layer may result which is composed primarily of  $\text{GaPO}_4$  and has good passivating properties over a GaAs substrate. Similarly, reported studies of plasma oxidation of aluminum film on GaAs (Reference 6) and  $\text{Ga}_{0.64}\text{Al}_{0.36}\text{As}$  (Reference 7), use of oxygen doped  $\text{Al}_x\text{Ga}_{1-x}\text{As}$  (Reference 8), and thermal oxidation of AlAs epilayers on GaAs (Reference 9) suggest that aluminum may also be a suitable species to incorporate into the GaAs surface for subsequent native oxide formation.

The initial phase of this program (Material and Native Oxide Development) concentrated on investigating the use of ion-implantation techniques to modify the GaAs surface with phosphorus for subsequent oxidation and formation of a device quality dielectric. Some effort was also spent upon investigating the use of aluminum implantation.

Section II presents a brief description of the ion implantation/oxidation approach for forming GaAs surface passivation layers, and discusses some of the aspects of this approach which are crucial in determining its applicability to the development of device quality insulators. Section III of the report describes the experimental procedures used and presents the results achieved. An assessment of these results relative to near-term application is given in Section IV.

## SECTION II

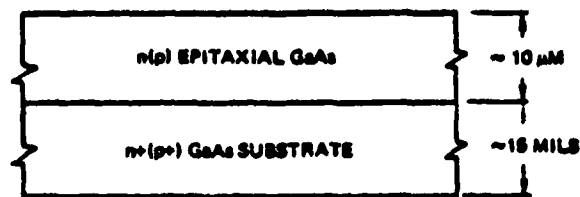
### NATIVE SURFACE PASSIVATION LAYER FORMATION ON GaAs USING ION-IMPLANTATION AND SUBSEQUENT OXIDATION

This section briefly describes the technical approach selected for investigation during this initial program phase, as well as the critical areas which must be evaluated in order to assess the feasibility of the approach. Experimental results are presented in Section III.

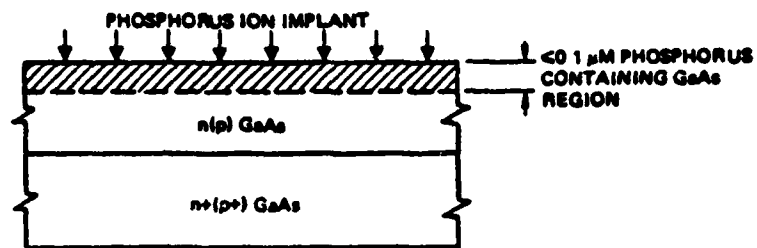
#### Basic Approach

Studies of the thermal oxidation of  $\text{GaAs}_{1-x}\text{P}_x$  (References 1, 2 and 5) have resulted in the formation of a native dielectric which may possess some properties suitable for MOS applications. In order to utilize the desirable properties of a dielectric formed in such a manner and still retain the high electron mobility of GaAs, it is desired to form a thin ( $\sim 0.05 - 0.10 \mu\text{m}$ ) phosphorus-containing surface layer which in turn can be oxidized to form the insulator. One method to form such a layer is through the introduction of phosphorus by ion implantation (Figure 1). This approach not only provides control over ion-dose (i.e., the phosphorus mole fraction,  $x$ , in  $\text{GaAs}_{1-x}\text{P}_x$ ) and ion-energy (thickness of the surface  $\text{GaAs}_{1-x}\text{P}_x$  layer), but is compatible with present semiconductor device manufacturing techniques.

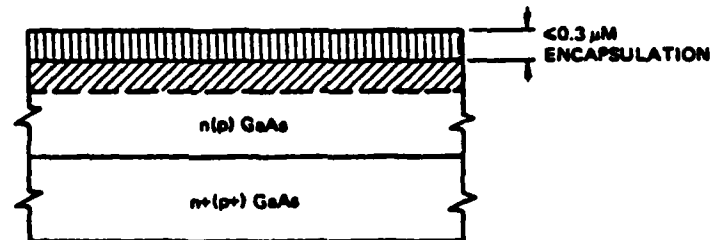




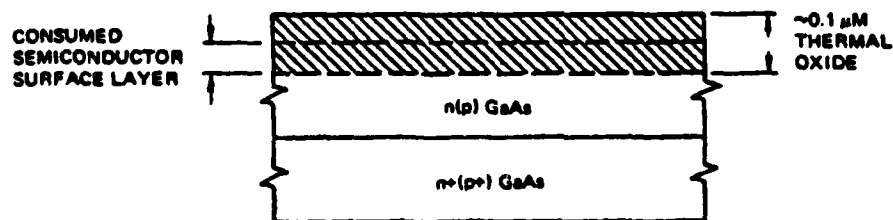
(a) STARTING MATERIAL IS LIGHTLY DOPED  $n$ - OR  $p$ -EPITAXIAL GaAs ON  $n^+$  OR  $p^+$  GaAs SUBSTRATE



(b) PHOSPHORUS ION-IMPLANTATION OF SELECTED ION ENERGY AND DOSE

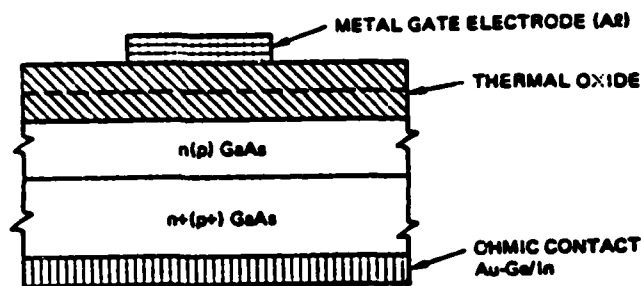


(c) OPTIONAL DEPOSITION OF ENCAPSULANT AND THERMAL ANNEALING IN  $H_2$  OR VACUUM (CAPLESS) ANNEAL. SUBSEQUENT REMOVAL OF ENCAPSULANT



(d) THERMAL OXIDATION OF PHOSPHORUS CONTAINING SURFACE LAYER

Figure 1. Process steps used to form a thermal oxide using phosphorus ion implantation



(e) METALLIZATION OF GATE ELECTRODE AND FORMATION OF OHMIC CONTACT TO  $n^+(p^+)$  SUBSTRATE AFTER LAPPING THE BACK SUBSTRATE SURFACE

Figure 1. (Cont.) Process steps used to form a thermal oxide using phosphorus ion-implantation

#### Synthesis of $\text{GaAs}_{1-x}\text{P}_x$ and $\text{Ga}_{1-x}\text{Al}_x\text{As}$ by Ion-Implantation into GaAs

Successful synthesis of ternary compound semiconductors by implantation of ions into solid substrates of binary compounds has been reported (References 10-13). Most of this work has involved the implantation of either aluminum or phosphorus into gallium arsenide. Belyi, et al (Reference 10) have reported formation of both  $\text{Ga}_{1-x}\text{Al}_x\text{As}$  and  $\text{GaAs}_{1-x}\text{P}_x$  using implant doses and energies of  $3.5 \times 10^{16}/\text{cm}^{-2}$  at 20 keV and  $5 \times 10^{16}/\text{cm}^{-2}$  at 30 keV, for phosphorus and aluminum ions, respectively. This latter work found that a hot substrate implant ( $420^\circ\text{C}$ - $500^\circ\text{C}$ ) was effective in synthesizing a relative defect-free ternary compound, as determined by luminescence spectra. Some of the aspects of the synthesis of  $\text{GaAs}_{1-x}\text{P}_x$  by implantation, and their relation to this program, are discussed below.

### Phosphorus Implantation Dose and Energy Considerations

The previous thermal oxidation work on  $\text{GaAs}_{1-x}\text{P}_x$  (References 1, 2, 4, 5) and GaP (References 14 and 15) has indicated that the presence of phosphorus in the starting semiconductor results in the formation of gallium phosphate ( $\text{GaPO}_4$ ) as one of the primary oxidation products. A comparison of the results of compositional depth profiles of the thermal oxides grown on several different binary compound semiconductors (Reference 15) indicated that only in oxides on gallium phosphide (GaP) are the elements perfectly oxidized. In the case of the present ion implantation approach, it is not known whether a high phosphorus mole fraction will be required to achieve a dielectric of sufficiently high quality. It is also not known whether all of the implanted species must be incorporated into the lattice before the same oxidation kinetics and reaction products result as with the previous single-crystal  $\text{GaAs}_{1-x}\text{P}_x$  experiments. With implanted phosphorus ions uniformly distributed in the surface layer and fully incorporated into the lattice structure to form single-crystal  $\text{GaAs}_{1-x}\text{P}_x$ , oxidation kinetics and products are expected to be similar to those of the previous work. The phosphorus concentration will not be uniformly distributed through the surface region using a single implant; however, a range of phosphorus percentage (e.g.,  $x = 0.2, 0.5$ , etc.) can be specified, which may result in oxides similar to those previously grown on single-crystal  $\text{GaAs}_{1-x}\text{P}_x$ .

Although it may be desirable to keep the phosphorus concentration in the surface region high to result in a maximum of gallium phosphate in the insulator, there are two reasons for keeping the phosphorus implant dose as low as possible. The first reason is that the electron mobility in  $\text{GaAs}_{1-x}\text{P}_x$  decreases as the phosphorus mole fraction is increased from  $x = 0$  to  $x = 1.0$ , with a sharp transition occurring at approximately  $x = 0.4$  (Reference 16). If

the entire phosphorus-containing layer is consumed during the oxidation step, then this problem will be alleviated because the semiconductor beneath the insulator will be gallium arsenide (i.e.,  $x = 0$ ). The second reason for using a lower phosphorus implant dose, if possible, is that any implantation-induced crystal lattice damage, if present, would be expected to be reduced. Based on these considerations, the initial investigations have been aimed toward formation of a surface layer which contains a phosphorus mole fraction range of  $0 \leq x \leq 0.4$ .

To calculate in a simplified manner the depth and the peak concentration of an implanted gaussian distribution (Figure 2), the projected range,  $R_p$ , of the implanted ions and the deviation about the mean,  $\Delta R_p$ , are required. The projected range statistics for phosphorus in gallium arsenide are not tabulated, and approximations must be used. It has been observed that with an atomic density correction, the results for a binary compound are indistinguishable from those of a target element whose atomic number is the average of those of the elements in the compound (Reference 17). Because the range statistics are directly proportional to atomic density, only a simple scaling factor is required in the conversion. In the present case, the tabulated range statistics for phosphorus in germanium ( $Z = 32$ ) will be used to approximate those for phosphorus in gallium arsenide [gallium ( $Z = 31$ ) and arsenic ( $Z = 33$ )]. The atomic density of Ge is  $4.42 \times 10^{22}$  atoms/cm<sup>3</sup>, and the molecular density of GaAs is  $2.21 \times 10^{22}$  molecules/cm<sup>3</sup> or  $4.42 \times 10^{22}$  atoms/cm<sup>3</sup> (Reference 18). Therefore, no scaling correction is required in this case. Table 1 gives the projected range statistics for selected implant energies of interest in this work.

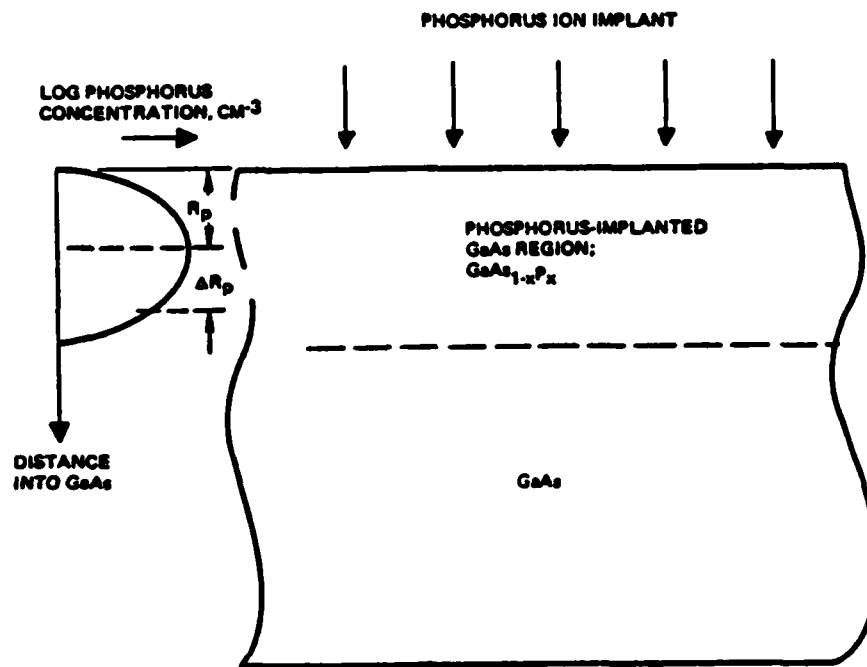


Figure 2. Phosphorus implant profile

Table 1. Projected Range Statistics for Phosphorus Implantation into Gallium Arsenide  
(Adapted from Reference 13)

Energy (keV)	Projected Range $R_p$ , ( $\mu\text{m}$ )	Projected Standard Deviation, $\Delta R_p$ , ( $\mu\text{m}$ )	Third Moment Ratio Estimate
20	0.0174	0.0116	0.322
30	0.0248	0.0158	0.270
40	0.0322	0.0198	0.223
50	0.0398	0.0236	0.181
60	0.0475	0.0273	0.141
80	0.0632	0.0344	0.071
100	0.0792	0.0412	0.008
120	0.0995	0.0476	-0.048
130	0.1037	0.0508	-0.074
140	0.1120	0.0538	-0.099
150	0.1203	0.0568	-0.122

The thickness of the phosphorus-containing surface region must be accurately controlled because it is desired that all or most of this layer be consumed during the oxidation step. Therefore, for this investigation the range of the implanted phosphorus ions is chosen to be limited to less than 0.1  $\mu\text{m}$ , which corresponds to an implant energy of less than approximately 130 keV for an uncovered GaAs surface. For surfaces coated with an encapsulation dielectric such as  $\text{SiO}_2$  or  $\text{Si}_3\text{N}_4$ , appropriate energy corrections must be made to take into account the thickness of such films.

With the projected range information available, approximations of the required ion implantation dose can be made. As an example, assume a  $\text{GaAs}_{1-x}\text{P}_x$  layer is to be formed with a phosphorus mole fraction of  $x = 0.33$ . Let it be assumed that all of the implanted phosphorus atoms are completely activated and that the replaced arsenic atoms are lost during high temperature annealing and/or oxidation steps. The molecular density of GaAs is  $2.2 \times 10^{22}$  molecules/ $\text{cm}^3$ , and because the number of gallium atoms must remain constant and available for bonding to the implanted phosphorus atoms to form the alloy, the gallium atom density is  $2.21 \times 10^{22}$  atoms/ $\text{cm}^3$ . If  $N_{\text{Ga}}$ ,  $N_{\text{As}}$ , and  $N_{\text{P}}$  are the atomic densities of gallium, arsenic, and phosphorus, respectively, then

$$N_{\text{Ga}} = N_{\text{As}} + N_{\text{P}} = 2.21 \times 10^{22} \text{ cm}^{-3}, \quad (1)$$

to form a stoichiometric alloy of  $\text{GaAs}_{1-x}\text{P}_x$ . It should be noted again that the originally present arsenic atoms which have been replaced by phosphorus are unaccounted for in this expression. In the present example of  $x = 0.33$ , then

$$N_{\text{As}} + N_{\text{P}} = (2N_{\text{P}}) + N_{\text{P}}, \quad (2)$$

$$\text{and } N_{\text{Ga}} = 3N_{\text{P}} \quad (3)$$

$$N_{\text{P}} = \frac{N_{\text{Ga}}}{3} = 7.35 \times 10^{21} \text{ atoms/cm}^3 \quad (4)$$

The implanted phosphorus ion dose required to produce  $7.35 \times 10^{21}$  atoms/cm<sup>3</sup> can be calculated assuming a gaussian distribution and using the simplified expression (Reference 17)

$$N_p \approx \frac{N_I}{2.5 \Delta R_p} \quad (5)$$

where  $N_p$  is the peak concentration/cm<sup>3</sup> in the implanted region,  $R_p$  is the projected standard deviation given in Table 1, and  $N_I$  is the implanted dose in ions/cm<sup>2</sup>. Therefore, if an energy of 50 keV is chosen ( $R_p \approx 475\text{\AA}$ ), then the required implant dose is approximately  $5.02 \times 10^{16}$  ions/cm<sup>2</sup>.

Table 2 gives the implant dose and energy values required to achieve several different phosphorus mole fractions of interest in the region of the implant peak. These values are for samples in which ions are implanted directly into the surface (i.e., not through an encapsulant).

Table 2. Phosphorus implant parameter values of interest

Peak Phosphorus Mole Fraction x	Implant Energy (keV)	Implant Dose (cm <sup>-2</sup> )	Approx. Implant Layer Thickness (Å) ( $R_p + \Delta R_p$ )
0.10	30	$8.73 \times 10^{15}$	400
	60	$1.51 \times 10^{16}$	750
	100	$2.28 \times 10^{16}$	1200
0.20	30	$1.75 \times 10^{16}$	400
	60	$3.02 \times 10^{16}$	750
	100	$4.56 \times 10^{16}$	1200
0.30	30	$2.62 \times 10^{16}$	400
	60	$4.53 \times 10^{16}$	750
	100	$6.84 \times 10^{16}$	1200
0.40	30	$3.49 \times 10^{16}$	400
	60	$6.04 \times 10^{16}$	750
	100	$9.12 \times 10^{16}$	1200
0.50	30	$4.37 \times 10^{16}$	400

As in silicon, device technology multiple implants of various energies can be used to tailor a relatively uniform phosphorus concentration throughout the surface layer. However, due to the long times required to achieve some of the higher implant doses initial experiments have investigated single implants.

#### Additional Considerations in Forming $\text{GaAs}_{1-x}\text{P}_x$ Layers

Phosphorus Implant Damage--The high-dose low-energy phosphorus implants are expected to result in the formation of an amorphous region near the semiconductor surface. Few experimental results are available for phosphorus implantation into GaAs. However, several other species have been implanted into GaAs, and the results from these experiments can be used to anticipate the behavior of the phosphorus implant. A post-implant high-temperature annealing treatment is generally required to electrically activate dopant species, such as Se, S, or Be, and to remove implant-induced crystal lattice damage. This annealing step is usually performed using an insulator encapsulant to avoid thermal decomposition of the GaAs surface. (Problems associated with this procedure are described later.)

The present situation is somewhat different because electrically active species are not being intentionally implanted. However, to provide a crystalline  $\text{GaAs}_{1-x}\text{P}_x$  surface layer whose structure is similar to that used in previous oxidation studies (References 1-5), it is expected that a post-implant anneal or hot substrate implant will be required. It is not known whether restructuring the semiconductor is even a necessary condition for forming a good quality insulator. The experimental results of this program, described later, indicate that recrystallization may not be required.



A recent publication (Reference 13) discusses the formation of defects created by phosphorus implantation into GaAs at doses of interest in this work. Rutherford backscattering analyses indicate that an amorphous surface layer resulted only for room temperature implants. However, defect distribution profiles extended deeper ( $400\text{\AA}$ ) into the substrate for implant temperatures up to  $400^{\circ}\text{C}$ . The total defect density decreased as the implantation temperature increased and this behavior was mainly due to a decrease in the surface defect density. The presence of the deeper defect profile tails was attributed to the acceleration of defect diffusion as a result of the irradiation. This assumption was supported by the fact that the defect profile tails were similar for both the hot and room temperature implants. A slightly earlier work (Reference 19) found, using cathodoluminescence, that no defect region existed under the phosphorus-implanted region. However, a defect region was found for the case of aluminum implanted into GaAs and its formation was attributed to excess gallium atoms being forced into the bulk of the crystal. In the case where a volatile (Group V) component is replaced, such as for phosphorus implantation, it was stated that the excess gallium required for reaction is probably formed by evaporation of the arsenic.

Because of the discrepancies in these earlier works, it is not known whether the formation of defects is a significant problem, particularly in the present case where it is desired to consume most or all of the implanted region during thermal oxidation. If defect regions extend deeply into the semiconductor, then deep traps or oxide-semiconductor interface states may result and degrade ultimate MOS device performance. The experimental investigation of possible amorphous-layer and defect-region formation, and the effects of both hot substrate implantation and post-implant annealing, is discussed later.

Post-Implant Encapsulation and Annealing--As mentioned earlier, an insulator is usually used to protect the gallium arsenide surface from thermal decomposition due to arsenic loss, during high-temperature post-implant annealing. The insulator usually used for encapsulation is silicon nitride ( $\text{Si}_3\text{N}_4$ ) (References 20-22), although silicon dioxide ( $\text{SiO}_2$ ) (References 23-25) and double layers of nitride/oxide (Reference 26) have also been investigated. In most cases the ions are implanted through the insulating layers and the samples are then annealed. In addition to the use of an encapsulant, several workers (References 27-29) have investigated capless annealing under various conditions.

The post-implant annealing temperature significantly influences the total disorder remaining after ion implantation, as described earlier. Because of the volatility of arsenic at the annealing temperatures required for crystal restructuring, both the structural quality and adherence properties of the deposited encapsulant are critical for maintaining surface stoichiometry.

Some workers (References 20, 23) have found that deposited  $\text{SiO}_2$  is unsuitable for encapsulation because gallium from the substrate tends to diffuse through the oxide. Other workers, however, (Reference 25) have found that  $\text{SiO}_2$  is as effective as  $\text{Si}_3\text{N}_4$  as an encapsulant. Recently, (Reference 26) annealing temperatures as high as  $1100^\circ\text{C}$  have been achieved using a  $\text{Si}_3\text{N}_4/\text{SiO}_2$  double layer. Although Nitride encapsulants are now commonly being used in GaAs device fabrication processes, a wide variety of effects, including adherence problems, cracking and blistering at high annealing temperatures, have been observed. The quality and repeatability of the annealing process appear to be very sensitive to both the surface preparation prior to encapsulant deposition, and the type of deposition process itself (e.g., plasma or sputtered). Also, little data exists for capping high dose implantations

of the type performed in this program. Because of the variable results reported in the literature and those obtained thus far in this program, it appears that the encapsulation/anncaling process is not fully understood and remains somewhat an art.

Few capless annealing results have been reported, and most of those which have been presented depend on a sealed tube and over-pressure of arsenic to minimize surface decomposition. These techniques do not appear to be suitable for large-scale device production. A recent result (Reference 29) in which uncapped implanted surfaces were in intimate contact with the surface of another GaAs wafer, indicates that there may be some hope for a simplified capless annealing procedure.

#### Oxidation Considerations

Oxidation Temperature and Time--The upper temperature limit for the growth of acceptable thermal oxides on  $\text{GaAs}_{0.5}\text{P}_{0.5}$  has been established as  $700^{\circ}\text{C}$  (Reference 1). More recent work (Reference 4) has indicated that a lower oxidation temperature reduces arsenic loss from the oxide and also results in lower dielectric leakage currents. Similar oxidation behavior to that observed previously would be expected in the case of an ion-implanted surface if the phosphorus concentration is uniform and crystallinity is completely restored by annealing. However, the effect on the oxidation behavior of the excess arsenic which must be replaced by the phosphorus is not known. In addition, the effects on the oxidation behavior of a nonuniform phosphorus concentration with depth, using a single implant, and the possibility of incomplete annealing are unknowns to be evaluated. Some results are given in a later section.

Oxide Thickness--The thickness of the grown oxide can be controlled by the ion-implant energy and subsequent high temperature processing steps. From the

results of thermal oxidation on bulk  $\text{GaAs}_{1-x}\text{P}_x$  (Reference 30) it is expected that the ratio of the thickness of the semiconductor consumed to that of the oxide grown is approximately 2/3. For example, to grow a 1000Å-thick oxide, the phosphorus-containing surface region must be approximately 700Å thick. This thickness then determines the selection of an ion implant which has a mean range of approximately 400Å into the GaAs. Therefore, from Table 1 it is seen that an energy of about 50 keV will be required for an implant into a bare GaAs surface.

Redistribution of Implanted Phosphorus--A final possible effect which must be considered is that of redistribution of the implanted phosphorus during both the annealing and oxidation steps. The diffusion of phosphorus in GaAs has been recently investigated (Reference 31). These workers observed a strong concentration-dependent increase in the diffusion coefficient at all temperatures from 800-1100°C, for phosphorus concentrations near  $\sim 10^{22}$  atoms/cm<sup>3</sup>. This value is in the concentration range of interest for forming  $\text{GaAs}_{1-x}\text{P}_x$ . At the lower annealing and oxidation temperatures (500-800°C) used in the present work, however, thermal redistribution is not expected to be a significant problem. The experimental results presented later tend to confirm this.

### SECTION III

#### RESULTS OF ION IMPLANTATION, ANNEALING, AND OXIDATION EXPERIMENTS

This section presents the results of ion implantation, post-implant annealing, and thermal oxidation experiments. These results are discussed with respect to those which were expected, and the problems associated with each process step are also described.

##### Starting Material and Surface Preparation

GaAs Starting Material--The initial ion-implantation experiments were conducted using (100) bulk n-type (Si-doped) GaAs wafers purchased from Monsanto and Crystal Specialties. The donor concentration specified by the manufacturer is  $7 \times 10^{17}$  to  $4 \times 10^{18} \text{ cm}^{-3}$ . The donor concentration determined from  $1/C^2$  vs. reverse bias voltage plots of Schottky diodes were in the range  $1$  to  $2 \times 10^{18} \text{ cm}^{-3}$ . The heavily doped bulk material is sufficient to provide the required baseline information needed for the implantation and oxidation growth experiments, although more lightly doped layers (epitaxial) will be needed for MOS device fabrication.

Substrate Surface Preparation--To prevent lifting and flaking of the implant encapsulant during high temperature processing, it is desirable that the GaAs surface be as clean and defect free as possible prior to the encapsulant deposition. To remove organic contaminants the GaAs surfaces underwent a solvent clean in trichloroethane, acetone, and deionized water. This clean was usually followed by a chemical etch to remove surface damage.

Because thinner ( $1\text{-}3 \mu\text{m}$ ) epitaxial films may be used for device fabrication, this etch step must be well controlled. To determine a solution with the most desirable characteristics for the present application, several component ratio

variations of the common GaAs etchant  $\text{H}_2\text{SO}_4:\text{H}_2\text{O}_2(30\%):\text{H}_2\text{O}$  were investigated. Many of these solutions left a visible, slightly grainy residual layer on the surface. These surfaces darkened after exposure to air for several days, indicating a surface chemical instability. The use of 'hot' etching solutions (i.e., freshly mixed) reduced this residue, but for many of the component ratios, high etch rates make them impractical for application to thin epitaxial layers.

Because the sulfuric acid-based etch solutions tend to result in somewhat unstabilized surfaces, a basic solution of  $20\text{NH}_4\text{OH}:7\text{H}_2\text{O}_2:973\text{H}_2\text{O}$  (Reference 32) was investigated. This solution has an etch rate of approximately  $1250\text{\AA}/\text{min}$  at room temperature, and the resulting surfaces do not exhibit a residual layer. Therefore, it was generally used for the surface polishing.

Many defects were visible in some of the early Monsanto starting material used in the chemical etching experiments. The etch step further delineated these defects, resulting in deep etch pits. Material received after discussions with the supplier displayed lower defect densities. In general, material obtained from another vendor (Crystal Specialties) has had a relatively low pit density following etching.

#### Ion Implantation

Implantations were performed using an Extrion Model 200-20 ion implanter. Phosphorus ion currents using this machine ranged from 1 to  $3\mu\text{A}$ , and implant times were typically 5 to 15 minutes to achieve the doses (e.g.,  $2 \times 10^{16}\text{cm}^{-2}$ ) desired for the annealing experiments. All samples were mounted intimately to the substrate holder using spring clips. The sample holder was then adjusted to an angle of  $7^\circ$  relative to the incident ion beam to prevent channeling along major crystallographic axes. During implantation a small region of each wafer was blocked off to prevent

implantation. This procedure allowed a direct comparison of the effects of the various annealing and oxidation steps on both the implanted and unimplanted areas.

### Encapsulation and Annealing Experiments

Silicon Nitride--Because of its wide use as an implant/annealing encapsulant, silicon nitride was initially investigated. Low-temperature rf-sputtered nitride films ( 3000Å thick) were deposited on GaAs surfaces which had been implanted with 100 keV phosphorus ions to a dose of  $1 \times 10^{16} \text{ cm}^{-2}$ . The samples were then annealed in forming gas at various temperatures for a period of one hour. Table 3 summarizes the results of these annealing procedures.

The sputtered nitride begins lifting and flaking between 600°C and 700°C. Oxides were grown on material annealed at 400°C-700°C using a thermal oxidation process at 550°C in dry oxygen for 30 minutes.

Table 3. Results of post-implant annealing experiments using sputtered  $\text{Si}_3\text{N}_4$  encapsulant ( $t = 3000\text{\AA}$ )

Annealing Temp. (°C)	Ambient	Time	Visual Results
400	Forming Gas	1 Hr.	No damage on nitride. No apparent surface damage after nitride removal.
500	Forming Gas	1 Hr.	Spots on nitride surface. No apparent damage after removal.
600	Forming Gas	1 Hr.	Holes appearing in nitride. Damaged regions following removal.
700	Forming Gas	1 Hr.	Nitride flaking and lifting. Damaged regions following removal.

Oxides grown on surfaces annealed at 400°C and 500°C exhibit an extremely heterogeneous appearance. At 600°C and 700°C annealing temperatures, the nitride begins to lift from the surface and the forming gas ambient apparently reacts with the exposed GaAs surface. For the material annealed at 700°C, about 30 percent of the area is observed to exhibit relative uniform oxide growth. This latter result seemed to indicate that higher temperature annealing is required to provide sufficient lattice reordering for oxide growth. The results of subsequent experiments on unannealed surfaces, however, show that this high-temperature anneal is not necessary to obtain the uniform oxide growth.

Because of the deleterious annealing properties of the sputtered nitride layers, low-temperature plasma nitride films were also investigated. The annealing results for these samples were essentially the same as those for the sputtered layers, with bubbling and lifting occurring at about 600°C.

In the annealing experiments described above, the nitride was deposited directly on the implanted GaAs surface. In silicon technology both  $\text{SiO}_2$  and  $\text{Si}_3\text{N}_4$  films are usually deposited on a thin thermally grown silicon dioxide film to improve adherence and achieve suitable interface properties. To determine if a similar procedure would improve the annealing properties of the nitride, samples were oxidized at 450°C in dry  $\text{O}_2$  for 1 hour. This procedure results in a native oxide thickness of approximately 140Å (Reference 33). Following oxidation, 1400Å of silicon nitride was sputtered onto the wafers, and phosphorus ions were implanted through both layers to a dose of  $1 \times 10^{16} \text{ cm}^{-2}$ . The ion energy (190 keV) was chosen such that the concentration peak of the implant lies at or near the semiconductor native oxide interface. After annealing at 600°C for just 30 minutes, bubbling and lifting of the nitride was observed. The bubbling is more severe



in the implanted regions of the wafers. This behavior is in contrast to that observed using silicon dioxide as an encapsulant, where significantly less damage occurred in implanted regions.

Based on the limited results obtained in this program, it appears that nitride is not an adequate encapsulant for annealing high dose implantation damage under our experimental conditions. Therefore, rather than expending an excessive amount of effort in perfecting nitride encapsulation procedures, silicon dioxide was explored as an alternate encapsulant.

Room Temperature Implantation and Annealing Variations using SiO<sub>2</sub>/Native Oxide Encapsulants--Our early experiments using silicon dioxide films which were chemically vapor deposited at 400°C onto bare GaAs surfaces indicated that lifting and decomposition of the underlying semiconductor occurred for annealing temperatures above about 650°C. Use of the thin ( $\sim 140\text{\AA}$ ) native oxide underneath the deposited SiO<sub>2</sub> layer, mentioned earlier in connection with silicon nitride films, has significantly improved the annealing characteristics. Therefore, use of these layers was investigated further because they seemed to hold more promise than the other capping layers.

Silicon dioxide layers of 1100-1300 $\text{\AA}$  were deposited over the 140 $\text{\AA}$  thick native oxide. Phosphorus ions were implanted through the encapsulants at energies ranging from 140 keV to 190 keV. Annealing was then carried out in dry nitrogen for one hour at various temperatures.

Surfaces annealed at 650°C showed broad faint rings under reflection electron diffraction (RED) analysis indicative of nonoriented polycrystalline and amorphous material. After a 750°C N<sub>2</sub> anneal for one hour, however, the surface yields an oriented single-crystal type of RED pattern with Kikuchi lines. These results

indicate that restructuring of the crystal is occurring at the surface between 700°C and 750°C.

Samples which had received an implant dose of  $3 \times 10^{16} \text{ cm}^{-2}$  did not display crystalline RED patterns up to an annealing temperature of 750°C, but instead displayed a pattern indicative of a polycrystalline layer over a single-crystal substrate. Therefore, it appears that a higher temperature is required to anneal surfaces implanted to the higher doses.

Attempts to anneal surfaces at 800°C have not been completely successful. Severe damage is observed, for example, after a 30-minute anneal at 800°C in  $\text{N}_2$  using a 1000Å-thick capping layer.

The decomposition occurs along crystallographic directions, and the films tend to lift around particles or defect regions. The maximum annealing temperature achieved to date ( $\sim 775^\circ\text{C}$ ) is below some that have been reported in the literature. Because the film quality (i.e., the presence of pinholes and inclusions) so critically affects the decomposition observed after annealing, it appears that the maximum annealing temperature can be raised with further improvements in film deposition processes and cleaning procedures.

The sampling depth of the diffracted electron beam used in the RED characterization is  $\sim 1500\text{\AA}$  in gallium arsenide. It should be noted that high-energy RED patterns only give a composite view of the surface region. To detect lower defect densities which may extend deeper into the substrate (Reference 13), a more sensitive technique, such as Rutherford (ion) backscattering, or possibly electroreflectance (Reference 34) should be used.

One significant and somewhat unexpected beneficial result of the high dose implant is its ability to greatly inhibit decomposition of the semiconductor under the

encapsulant during high temperature annealing. This effect is illustrated in the photomicrograph of Figure 3, which shows the boundary between an unimplanted region and a region which had been implanted to a dose of  $1 \times 10^{16} \text{ cm}^{-2}$ . This sample was annealed at  $725^\circ\text{C}$  for 1 hour in  $\text{N}_2$ , followed by removal of the  $\text{SiO}_2$ . The damage (gallium flow) areas on the unimplanted side abruptly end at the implant boundary. This behavior contrasts with that which occurs when using a nitride encapsulant. The reason for this difference may be due to differences in the tensile or compressive stresses occurring at the insulator-semiconductor interface.



Figure 3. Boundary between implanted and unimplanted region following anneal at  $725^\circ\text{C}$  using  $\text{SiO}_2$  encapsulant (247X)

High-Temperature Implantation Using  $\text{SiO}_2$  Encapsulant--It has been observed that by elevating the temperature of the GaAs substrate during the implantation, significantly lower lattice damage levels result due to thermal annealing. To examine this effect, implantations were performed on substrates whose temperatures were held at either  $300^\circ\text{C}$  or  $400^\circ\text{C}$ . Higher temperature implantations could not be achieved because of substrate heater element failure above  $400^\circ\text{C}$ .

Table 4. Hot-substrate implant variations  
 $t_{\text{SiO}_2} \approx 1000\text{\AA}$ ,  $t_{\text{no}} \approx 140\text{\AA}$ ,  $E_p = 140 \text{ keV}$

Implant Dose ( $\text{cm}^{-2}$ )	Implant Temp. ( $^{\circ}\text{C}$ )	Reflection Diffraction Patterns
$1 \times 10^{16}$	300	Broad rings and faint Kikuchi lines
$2 \times 10^{16}$	300	Broad rings and faint Kikuchi lines
$2 \times 10^{16}$	400	Broad rings and faint Kikuchi lines

Table 4 lists the 'hot' implant variations attempted during the program. Electron diffraction patterns were made of the surfaces following removal of the capping layers. The results were similar for all variations and indicative of a polycrystalline layer of nonpreferred orientation over single-crystal material. Diffraction patterns were also made as a function of depth by chemically removing the surface region. For the first case listed in Table 4, the patterns show increasingly strong Kikuchi lines with depth, indicating that significant damage does not extend deeply into the substrates. The RED patterns for the hot implants are similar to those for room temperature implants which subsequently underwent annealing at  $725\text{--}750^{\circ}\text{C}$ . However, oxides grown on the 'hot' samples are generally inferior to those grown on samples implanted at room temperature. This result will be discussed further in the next section.

#### Oxidation Experiments Phosphorus Implanted GaAs

The oxidation experiments with phosphorus implanted GaAs have generally borne out our hypothesis that the GaAs surface can be suitably modified by implantation to prevent decomposition during oxidation and to promote a structurally more desirable oxide than on the unmodified surface. For most of the results reported here, an oxidation temperature of  $500^{\circ}\text{C}$  was chosen based upon results

achieved on bulk  $\text{GaAs}_{1-x}\text{P}_x$  (Reference 4).

A representative example indicating the contrast between oxides achieved over implanted and unimplanted regions on the same GaAs wafer is shown in Figure 4.

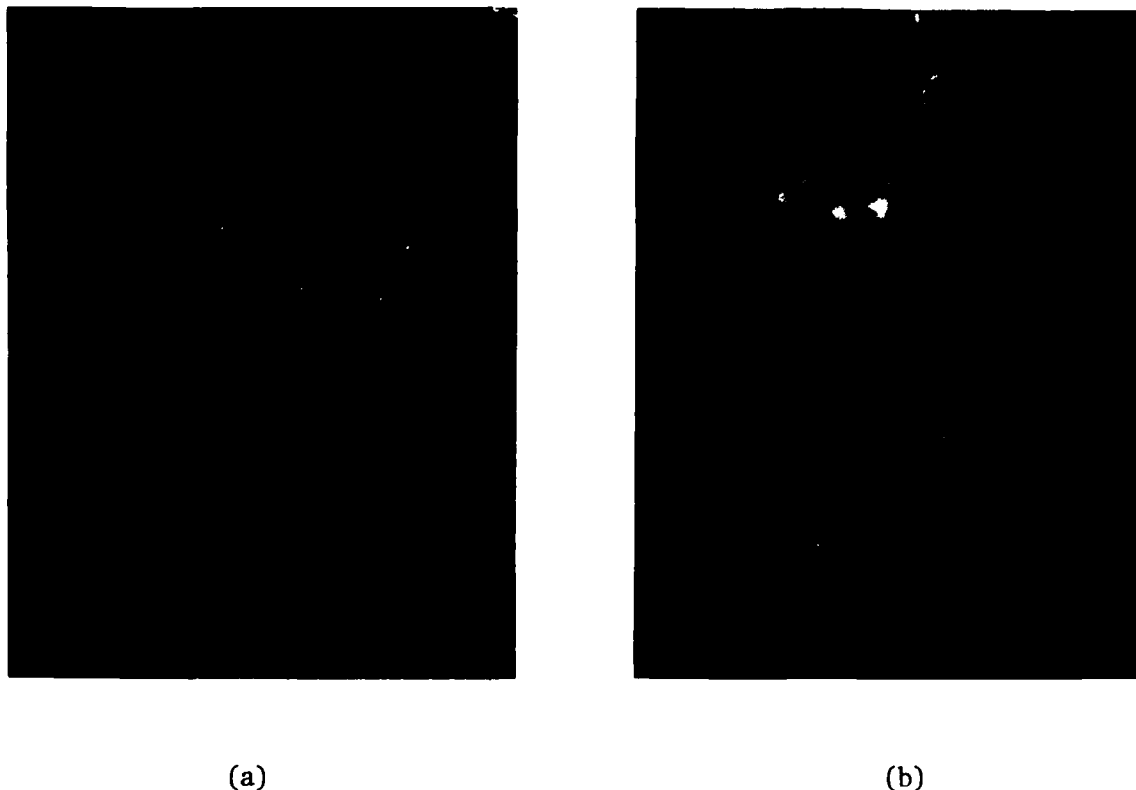


Figure 4. Photomicrograph of oxide surface (247X), (a) regions of GaAs implanted with  $1.8 \times 10^{16} \text{ cm}^{-2} \text{ }^{31}\text{P}^+$  at 190 keV and annealed with silox encapsulant at  $725^\circ\text{C}$ ,  $\text{N}_2$ , 1 hr.; (b) unimplanted region same wafer.

The oxide film was grown in dry  $\text{O}_2$  at  $600^\circ\text{C}$  for 30 minutes. The film over the implanted region visually appears less heterogeneous than any of those which have previously been grown on bulk  $\text{GaAs}_{1-x}\text{P}_x$  (References 3 and 4). On the other hand, the oxide grown over the unimplanted region of the same wafer shows evidence

of decomposition and gallium flow. The conditions under which results such as this are achieved were studied over a limited range of implant conditions (dose, energy, temperature) and encapsulants (capped and uncapped).

#### Oxidation of SiO<sub>2</sub>-encapsulated and Annealed Surfaces

Annealing Temperature Effects--Samples annealed at various times and temperatures under silox encapsulant were oxidized at 600°C in dry oxygen. For wafers implanted at room temperature to  $1 \times 10^{16}/\text{cm}^2$ , 190 keV and annealed at 750°C for 30 minutes, or 725°C for one hour, uniform oxide films were observed with decomposition only along wafer edges and around defect areas originally present in the material. Regions of wafers which were blocked off during implantation (i.e., gallium arsenide regions) exhibited uniform oxide growth in some areas but significant decomposition and gallium bubbling in other areas. Results shown in Figure 4 were typical. Surfaces annealed at 750°C had a more nonuniform film but no gallium bubbling. Progressively worse results were achieved for oxidized surfaces over regions annealed at temperatures lower than 725°C. Figure 5 shows the oxidized surface of a sample annealed at 650°C for 1 hour. Decomposition and gallium bubbling is observed in several regions with uniform growth in other areas.

Implant Dose Effects--Oxidation of annealed (725°C) surfaces at 600°C for 2.5 hours in O<sub>2</sub> yielded oxide thicknesses of about 600Å for a dose of  $1 \times 10^{16} \text{ cm}^{-2}$  and 900Å for  $3 \times 10^{16} \text{ cm}^{-2}$ , as determined using a Dektak surface profiler. These values compare to an oxide thickness of 400-500Å grown over the unimplanted (i.e., GaAs) areas. The previous oxidation studies of crystalline GaAs<sub>1-x</sub>P<sub>x</sub> (References 2, 4, 5) had shown that the growth rate of oxides decreases for increasing phosphorus content in the semiconductor. However, the behavior in the present



Figure 5. Surface following annealing at 650°C in N<sub>2</sub>, 1 hr. and oxidation at 600°C, 30 min., (SiO<sub>2</sub> encapsulant (97X)

case, for implanted surfaces, is opposite to this. The difference in oxidation kinetics may be due to incomplete annealing of implant-induced lattice damage. Also, as described later, the single phosphorus implant results in a nonuniform concentration of oxide constituents as a function of depth. Thus, oxidation rates would also be expected to be complicated and to vary with depth.

The dose levels investigated thus far ( $1-3 \times 10^{16} \text{ cm}^{-2}$ ) result in low phosphorus mole fractions ( $0.03 \leq x \leq 0.10$ , according to Eq. (5), after implantation through the capping layer. Although higher phosphorus levels may be desirable to obtain an increased gallium phosphate (GaPO<sub>4</sub>) content in the oxide

layer, initial indications are that optimum growth results may occur at doses less than  $3 \times 10^{16} \text{ cm}^{-2}$  for the annealed samples. Wafers which had received  $3 \times 10^{16}$  phosphorus ions/ $\text{cm}^2$ , followed by annealing at  $725^\circ\text{C}$ , yielded very grainy surfaces upon oxidation at  $600^\circ\text{C}$ , as shown in Figure 6. Oxides grown on surfaces which had lower implant levels exhibited significantly less graininess, as did oxides grown on unannealed surfaces at the higher dose levels.

Hot Implants--Oxides grown on surfaces which had received elevated-temperature implantations were generally nonuniform and of poor quality. Figure 7 shows the oxide grown at  $600^\circ\text{C}$  on a sample which had a dose of  $1 \times 10^{16}$  ions/ $\text{cm}^2$  implanted through a silicon-dioxide encapsulant at  $400^\circ\text{C}$ . In this case darker spots of oxide are surrounding particle-like nucleation centers. It is possible that this may be caused by an interaction between the gallium arsenide surface and the silicon dioxide used as an encapsulant. It should be noted, however, that a  $750^\circ\text{C}$  anneal following room-temperature implantation did not result in this behavior.

The oxides grown on samples implanted at  $300^\circ\text{C}$  show damage similar to that occurring for room temperature implants annealed at lower temperatures (e.g., Figure 5). Encapsulated samples which were annealed at  $725^\circ\text{C}$  following the hot implant have exhibited somewhat better quality oxides than those without post-(hot)-implant anneal. These films, however, are still not the quality of those grown on either the room-temperature implanted and high-temperature annealed or the unencapsulated/unannealed samples to be discussed later.

Implant Energy Effects--Some regions of the samples implanted at 190 keV showed decomposition after oxidation. With this implant energy, the projected range of the implanted ions is approximately  $700\text{\AA}$  into the GaAs (i.e., after





Figure 6. Nomarski photomicrograph of oxide grown on annealed implanted surface (Dose:  $3 \times 10^{16} \text{ cm}^{-2}$ ) (280X)

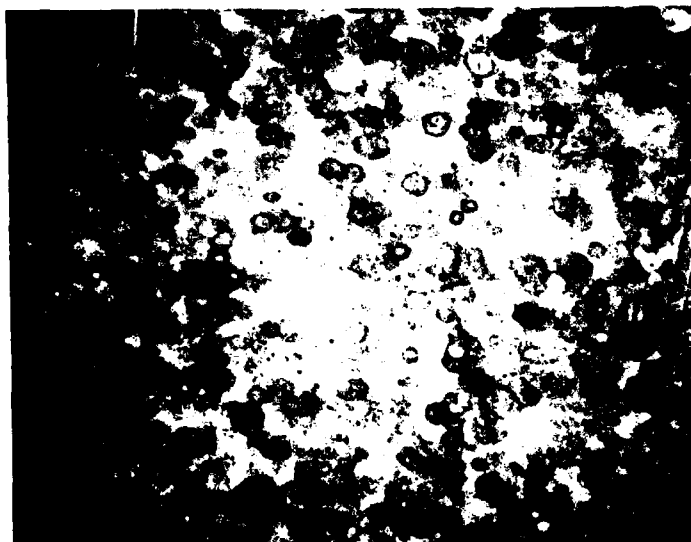


Figure 7. Oxide grown on surface implanted at  $400^{\circ}\text{C}$  ( $\text{SiO}_2$  encapsulant) (247X)

passing through the  $\text{SiO}_2$  encapsulant). It appears that the phosphorus concentration at the GaAs surface may be too low with the 190 keV implant energy. Therefore, an implant energy of 140 keV was also investigated on samples with the same  $\text{SiO}_2$  thickness ( $\sim 1100\text{\AA}$ ). With this energy, the projected range of the peak is at a depth approximately  $300\text{\AA}$  from the GaAs surface. Oxides grown on these surfaces show fewer areas of decomposition than those with the higher energy, indicating that surface phosphorus concentration is critical. The oxidation results on unannealed surfaces also showed that location of the implant peak is important in determining oxide quality. This point is described below.

#### Oxidation of Unannealed Implanted Surfaces

In order to determine if high-temperature annealing using an encapsulant is required to achieve high-quality and uniform oxide growth, samples were oxidized after phosphorus had been implanted directly into the GaAs surfaces. Generally, implant parameter variations have duplicated those used for encapsulated samples.

One concern about low-energy high-dose implantation into a bare GaAs surface is the possible sputtering which may result. To examine if this effect was significant for the phosphorus implants, Dektak surface profile measurements were made across implanted and unimplanted boundary regions. No step could be detected up to the maximum sensitivity ( $< 100\text{\AA}$ ) of the instrument. Therefore, it appears that sputtering effects are not significant for these implant conditions.

Implant Dose Effects--Implant doses ranging from  $6 \times 10^{15}\text{cm}^{-2}$  to  $3 \times 10^{16}\text{cm}^{-2}$  were investigated. The implant energy used for these experiments was fixed at 60 keV. Table 5 summarizes the effects of these dose variations. A dose of  $6 \times 10^{15}\text{cm}^{-2}$  is apparently too low to result in uniform oxide growth, and areas

Table 5. Results of Phosphorus Ion Dose Variations for Unannealed Surfaces (60 keV, Room Temp. Substrate). Oxidation: 600°C, O<sub>2</sub>

Dose (cm <sup>-2</sup> )	Oxidation Time (Hr.)	Approx. Oxide Thickness (Å)	Remarks
6 x 10 <sup>15</sup>	0.5	400	Decomposition near wafer edge
	1.5	550	Slightly grainy, slight decomp.
	2.5	600	Areas of decomposition
1.8 x 10 <sup>16</sup>	0.5	400	Uniform, no damage
	1.5	550	Uniform
	2.5	625	Uniform, minimal damage
3 x 10 <sup>16</sup>	0.5	650	Slightly grainy, scattered white spots
	1.5	800	Uniform, a few small spots
	2.5	900	Same as above

of decomposition are scattered about the surface. Medium-dose implants (1-2 x 10<sup>16</sup> cm<sup>-2</sup>) generally result in uniform oxides with little or no decomposition apparent. Films grown in this dose regime display only slight structure (graininess) similar to that observed in thermal oxides grown on GaAs<sub>1-x</sub>P<sub>x</sub> at the same temperature. An implant dose of 3 x 10<sup>16</sup> cm<sup>-2</sup> yields thicker uniform oxides than the lower doses, but there are a few very small white 'particle-like' spots interspersed in the oxide matrix. These spots do not appear to be nucleation regions for decomposition.

Implant Energy Effects--The effects of implant energy were investigated at a fixed ion dose of 1 x 10<sup>16</sup> cm<sup>-2</sup>. After implantation, samples were oxidized in O<sub>2</sub> at 600°C for 5 hours. Implants at 100 keV and 150 keV (R<sub>p</sub> ≈ 790 Å and

1200Å, respectively) resulted in nonuniform oxide growth with a banding similar to that which is observed when GaAs rapidly oxidizes. This effect is illustrated in the photomicrograph of Figure 8.



Figure 8. Oxide Growth on Unannealed Surface  
Implanted at 150 keV ( $1 \times 10^{16} \text{ cm}^{-2}$ )  
(247X)

The low-energy implants at 30 keV and 60 keV (with  $R_p \approx 250\text{\AA}$  and  $475\text{\AA}$ , respectively) generally resulted in smooth oxides of uniform thickness. There was decomposition migrating inward from the wafer edges (Figure 9). This is believed to be due to the exposure of the unimplanted wafer edge during oxidation.



Figure 9. Oxide Growth on Unannealed Surface  
Implanted at 30 keV ( $1 \times 10^{16} \text{ cm}^{-2}$ )  
(481X). (Boundary between uniform  
oxide and decomposed strip around  
wafer edge.)

The results of the implant energy variations indicate, as do those for the  $\text{SiO}_2$ -encapsulated and annealed samples, that the implant peak should be close to the semiconductor surface to avoid damage during oxidation. It may not necessarily be true that the lowest energy implants result in higher quality oxides. Comparison of higher dose ( $3 \times 10^{16} \text{ cm}^{-2}$ ) implants indicates a larger degree of structure and graininess in oxides grown on surfaces implanted at 60 keV.

Hot Implants--Oxide films which were grown on 'hot-implanted' samples were of a quality comparable to those grown on surfaces implanted at room temperature. No surface decomposition was visible up to an implant temperature of  $400^\circ\text{C}$ . There was, however, a difference in oxide thickness noted between room temperature and hot implant samples which had received the same

implant dose and oxidation temperature and time. For a phosphorus ion dose of  $2 \times 10^{16} \text{cm}^{-2}$  and an oxidation time and temperature of 2.5 hours at  $600^\circ\text{C}$  in  $\text{O}_2$  the resulting film thicknesses were approximately  $700\text{\AA}$  and  $1000\text{\AA}$  for room temperature and  $400^\circ\text{C}$  implants, respectively. The reason for this difference is not known. If the high temperature implant results in less lattice damage, as expected, then a lower oxide growth rate would also be expected.

#### Aluminum Implanted GaAs

A few experiments were conducted to investigate the implantation of aluminum into GaAs and the subsequent oxidation of the implanted surfaces. Doses of  $1.5 \times 10^{16} \text{cm}^{-2}$ ,  $3 \times 10^{16} \text{cm}^{-2}$ , and  $5 \times 10^{16} \text{cm}^{-2}$ , implanted directly into the GaAs surface at an energy of 50 keV, were examined. These doses correspond to approximate aluminum mole fractions in  $\text{Ga}_{1-x}\text{Al}_x\text{As}$  of  $x = 0.1$ ,  $x = 0.2$ , and  $x = 0.33$ , respectively. These dose levels are also comparable to those studied for phosphorus. Following implantation, the surfaces were oxidized at  $600^\circ\text{C}$  in  $\text{O}_2$  for times ranging from 30 minutes to 120 minutes. In all cases the implanted surfaces decomposed upon oxidation, with numerous areas indicative of gallium flow (Figure 10).

The feasibility of using encapsulation and subsequent annealing was also investigated. Samples with a CVD- $\text{SiO}_2$  layer approximately  $1000\text{\AA}$  in thickness were implanted with 130 keV aluminum ions at doses of  $3 \times 10^{16} \text{cm}^{-2}$  and  $4 \times 10^{16} \text{cm}^{-2}$ . These samples were then annealed in  $\text{N}_2$  at  $650^\circ\text{C}$  for 1 hour. Figure 11 is a Nomarski interference contrast photomicrograph of the boundary between the implanted and unimplanted regions following annealing. The silicon dioxide layer has lifted and decomposition is occurring even at this relatively low temperature. This behavior contrasts with that observed for phosphorus implanted surfaces where annealing temperatures up to  $800^\circ\text{C}$  have been successful.

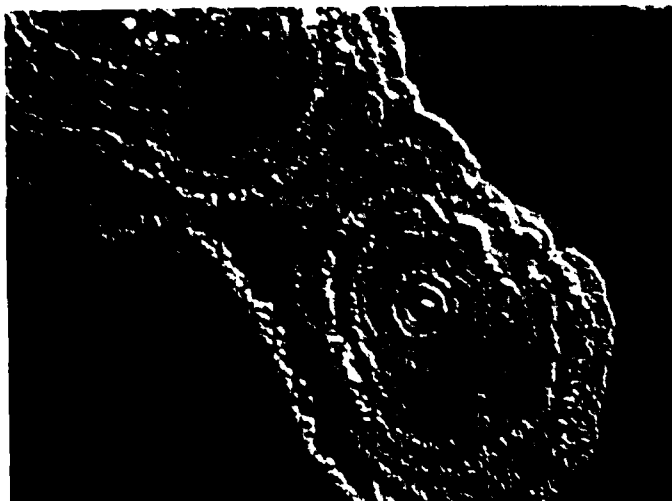


Figure 10. Nomarski photomicrograph of damage following oxidation of aluminum implanted surface ( $5 \times 10^{16} \text{cm}^{-2}$ , 50 keV) with dry  $\text{O}_2$  for 2 hours at  $600^\circ\text{C}$  (151X)



Figure 11. Nomarski photomicrograph of boundary between implanted and unimplanted regions following  $650^\circ\text{C}$   $\text{N}_2$  anneal with  $\text{SiO}_2$  encapsulant (151X)

The reason for the difference in oxidation behavior between the unannealed phosphorus-implanted and aluminum-implanted surfaces is not known. If the aluminum ions were incorporated into the lattice structure to form  $\text{Ga}_{1-x}\text{Al}_x\text{As}$ , it would be expected that the excess gallium displaced from the original lattice would be present during oxidation to react with oxygen to form  $\text{Ga}_2\text{O}_3$ . In forming  $\text{GaAs}_{1-x}\text{P}_x$  by phosphorus implantation, free arsenic would be expected. This arsenic could combine with oxygen to form volatile reaction products, such as  $\text{As}_2\text{O}_3$ .

Satisfactory annealing of aluminum-implanted surfaces may require a higher quality encapsulant than that required for phosphorus-implanted surfaces. Annealing with a higher quality  $\text{SiO}_2$  or  $\text{Si}_3\text{N}_4$  encapsulant than has been obtained to date is indicated.

Although there are some additional experiments which can be performed with aluminum-implanted samples (e.g., hot implants and annealing with improved encapsulant), these initial results indicate that determining the optimum implantation, annealing and oxidation conditions may take time that is outside the scope of this program. Hence, no further work on this approach was pursued.

#### MIS Capacitor Experiments

Electical characterization has been performed on MIS capacitors formed on some of the better quality films. Figures 12 and 13 show C-V characteristics of implanted and unimplanted devices, respectively, whose oxides were grown at  $600^\circ\text{C}$  in dry  $\text{O}_2$ . The implanted oxide exhibits hysteresis and deep depletion somewhat similar to oxides grown on single-crystal  $\text{GaAs}_{1-x}\text{P}_x$ . The  $(\Delta C/\Delta V)$  of this curve is lower than that expected for the specified donor concentration,



- (1) 0 → -8  
(2) -8 → +2

CONTRACT AFAL  
LOT/WAFER 841-2E-7 (II)  
DATE/BY 2/25/79  
 $N_d \sim 5 \times 10^{16} \text{ cm}^{-3}$   $f = 1 \text{ MHz}$   
 $A \approx 4.0 \times 10^{-3} \text{ cm}^2$   $t_{\text{ox}} \approx 800 \text{ \AA}$

$\phi \sim 2 \times 10^{16} \text{ cm}^{-2}$   
~310°C S.S. During Implant  
600°C, O<sub>2</sub>, 3 Hr.

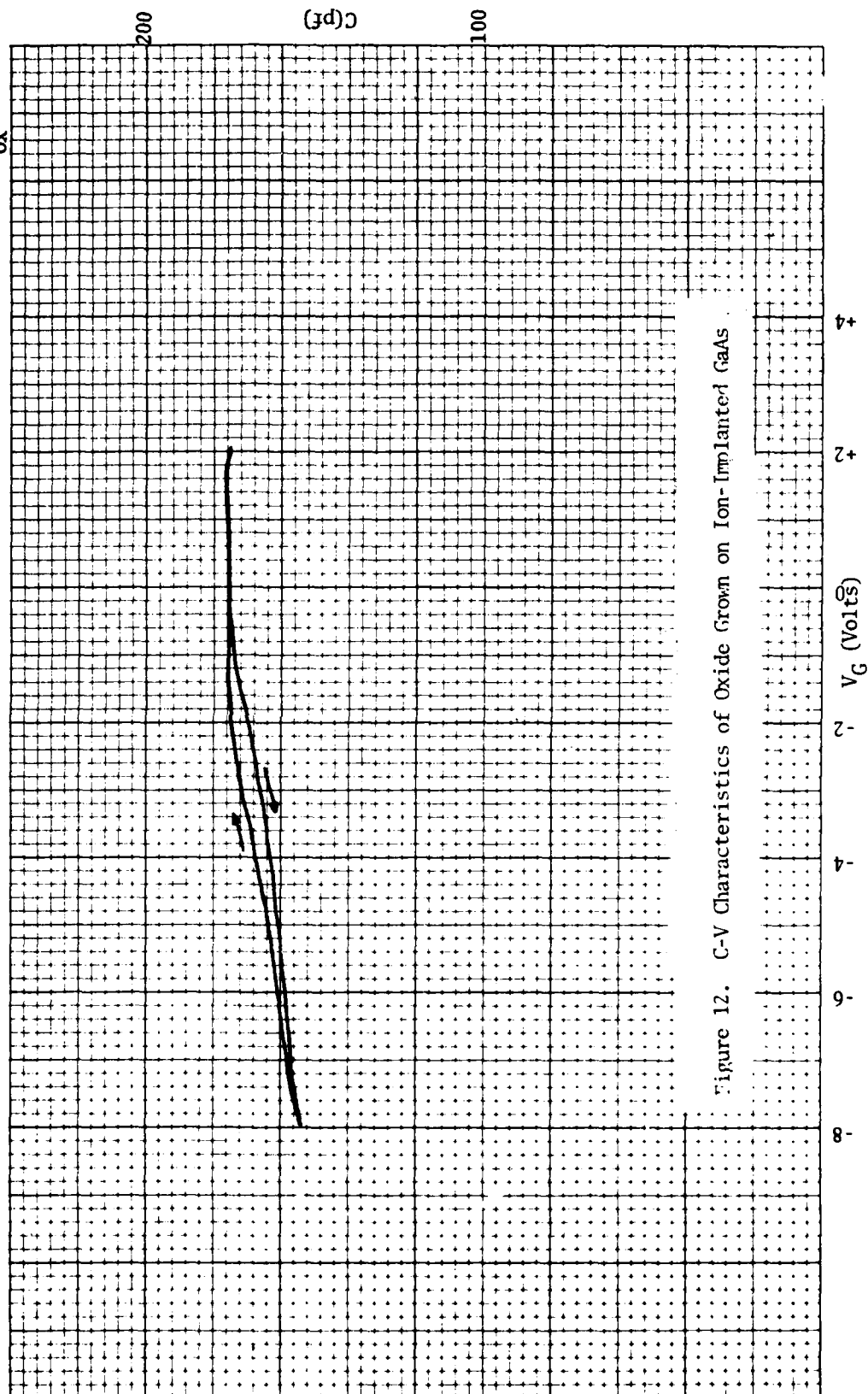


Figure 12. C-V Characteristics of Oxide Grown on Ion-Implanted GaAs

- (1) 0 → +2
- (2) 2 → -9
- (3) 9 → +2

CONTRACT AFAL  
 LOT/WAFER 841-2E-9 (UI)  
 DATE/BY 2/25/79  
 $N_D \sim 5 \times 10^{16} \text{ cm}^{-3}$   $f = 1 \text{ MHz}$   
 $A \approx 3.5 \times 10^{-3} \text{ cm}^2$   $t_{\text{ox}} \approx 650 \text{ \AA}$

600°C, O<sub>2</sub>, 3 Hr.  
 GaAs

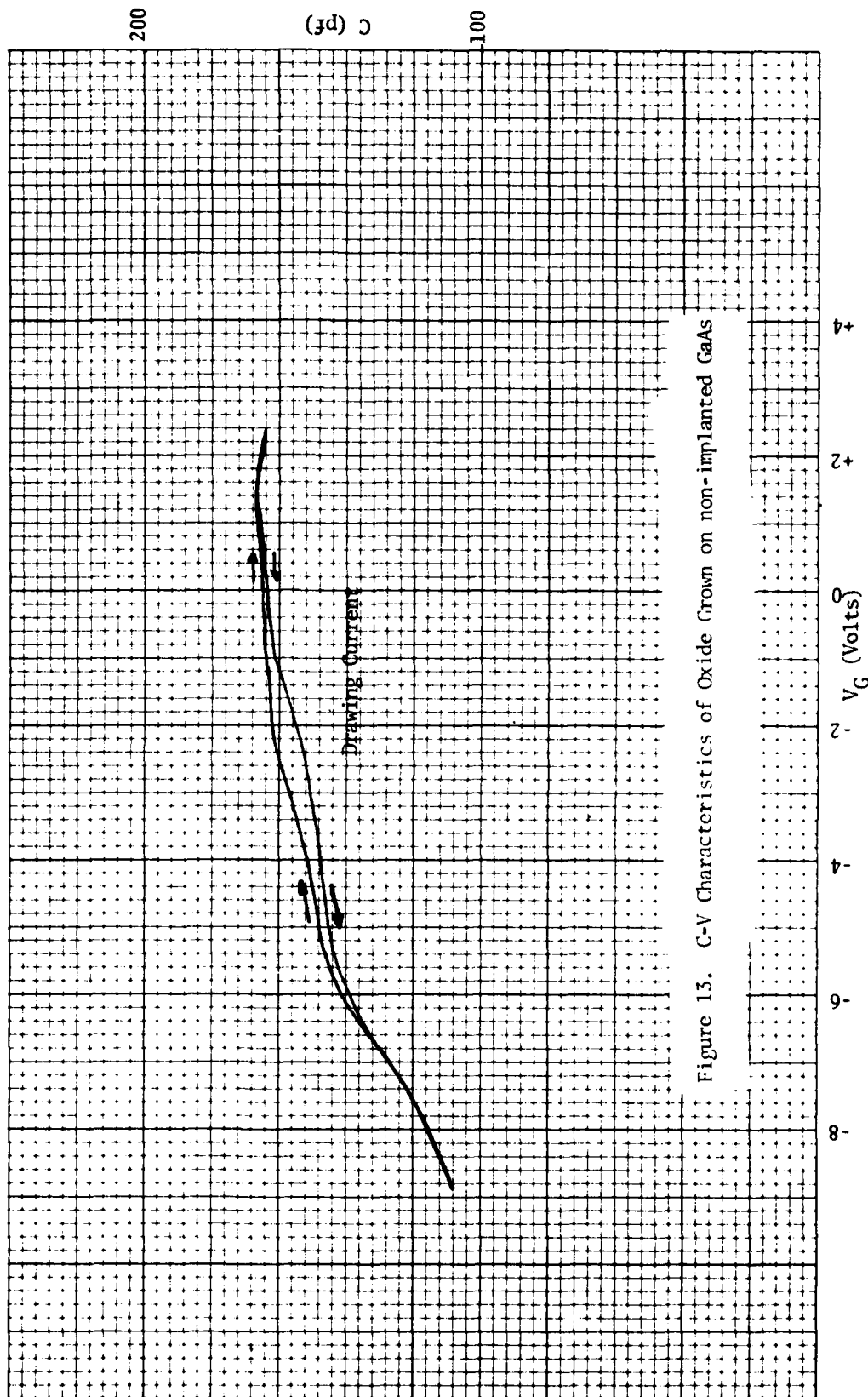


Figure 13. C-V Characteristics of Oxide Grown on non-implanted GaAs

and could indicate possible charge trapping under the insulator due to incomplete annealing of lattice damage. The unimplanted devices indicated excessive leakage in both forward and reverse bias directions. Initial d-c leakage current measurements (Figure 14) indicated that the leakage is comparable for the thicker ( $\sim 600\text{-}900\text{\AA}$ ) phosphorus-implanted and unimplanted films. However, the thinner ( $\sim 400\text{-}500\text{\AA}$ ) unimplanted oxides exhibited more leakage current for a given electric field than the oxide grown over implanted areas. These leakage current densities are greater than those for oxides grown on  $\text{GaAs}_{1-x}\text{P}_x$  and further optimization of the annealing processes are indicated.

It should be noted that the unimplanted oxides are difficult to chemically remove and only approximate measurements of thickness can be made for these films. Implanted films are somewhat easier to remove (using buffered HF) and surface profile; however, due to nonuniform composition, variable results have been achieved on these layers.

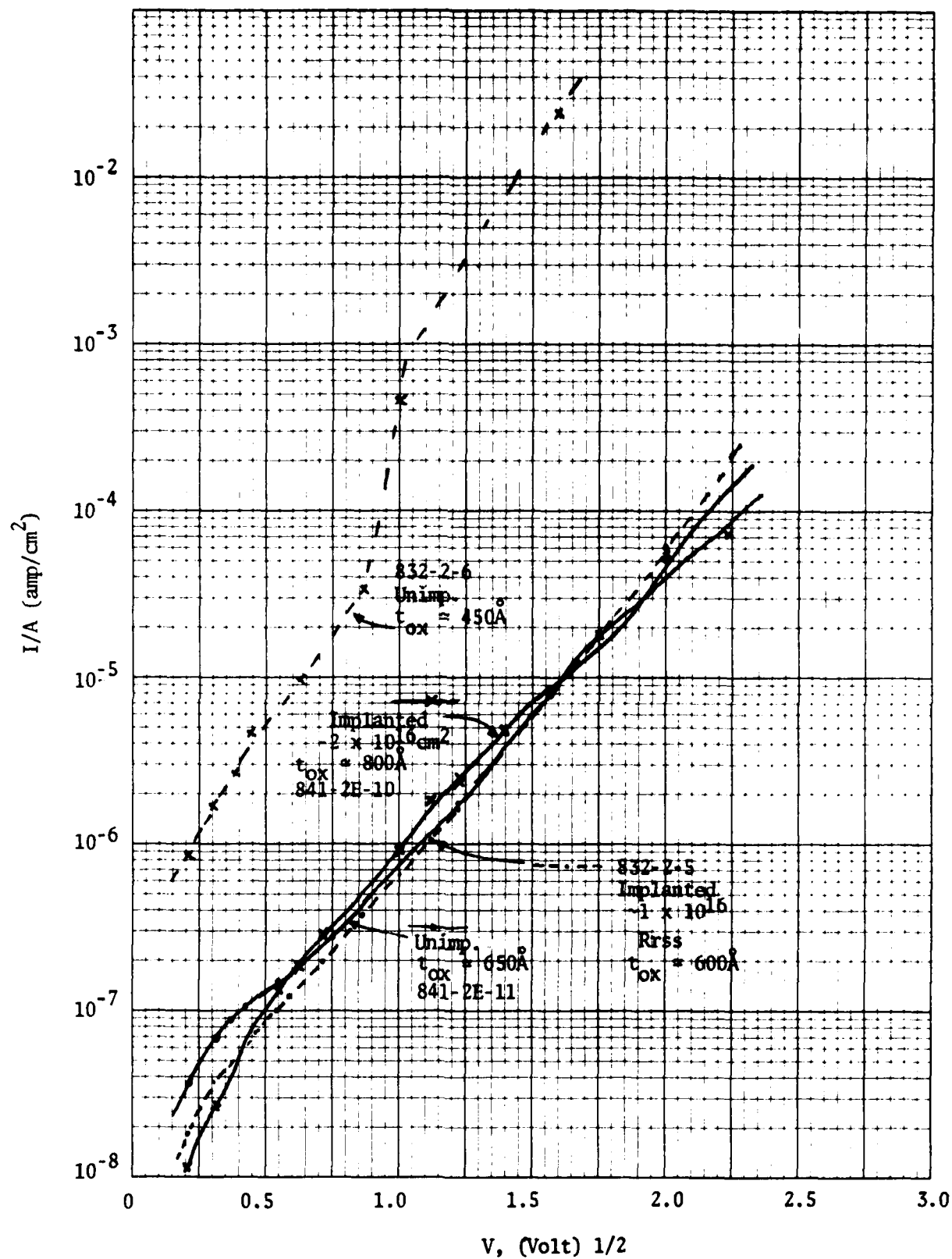


Figure 14. DC Current-Voltage Characteristics of Thermal Oxides on GaAs

### Ion Microprobe Analysis of Implant Profiles and Oxide Composition

Ion microprobe mass analysis (IMMA), fundamentally secondary ion mass spectrometry (SIMS) analysis of microarea regions, was used to examine the elemental depth composition of some of the ion implanted and oxidized surface layers. Depth profiles were obtained with an ARL IMMA using a primary beam of  $^{18}\text{O}_2^+$  ions with a beam energy of 20 keV. Details of this analytical technique and its limitations are given in References 4 and 35.

Figures 15 (a) and (b) show IMMA profiles for  $\text{SiO}_2$ -encapsulated/implanted samples before and after annealing respectively. For comparison, an ideal LSS implant profile is included in Figure 15 (a). This simplified ideal profile neglects third-moment effects, which can sometimes skew the profile about the implant peak (Reference 17).

The sample of Figure 15 (b) had a 5 second surface etch to remove a slight residue. Although there is a slight sputter rate (therefore, ion yield) difference between the two samples in Figure 15 (a) and (b), some comparisons can be made. There is apparently no significant diffusion of phosphorus into the substrate following annealing at 725°C. The phosphorus profile tails of both samples appear to extend somewhat deeper into the substrate than expected from LSS theory. It is believed that this is not necessarily enhanced diffusion during the implant, but rather a 'knock-in' effect which occurs when light mass elements are sputtered using a high energy beam (Reference 31). With analytical techniques which use lower sputtering beam energies, such as the Auger and ESCA measurements this 'knock-in' should be reduced to some extent.

The rapid increase in arsenic and phosphorus counts near the surface is another artifact of this technique, and is due to the establishment of equilibrium conditions during sputtering with the oxygen beam.

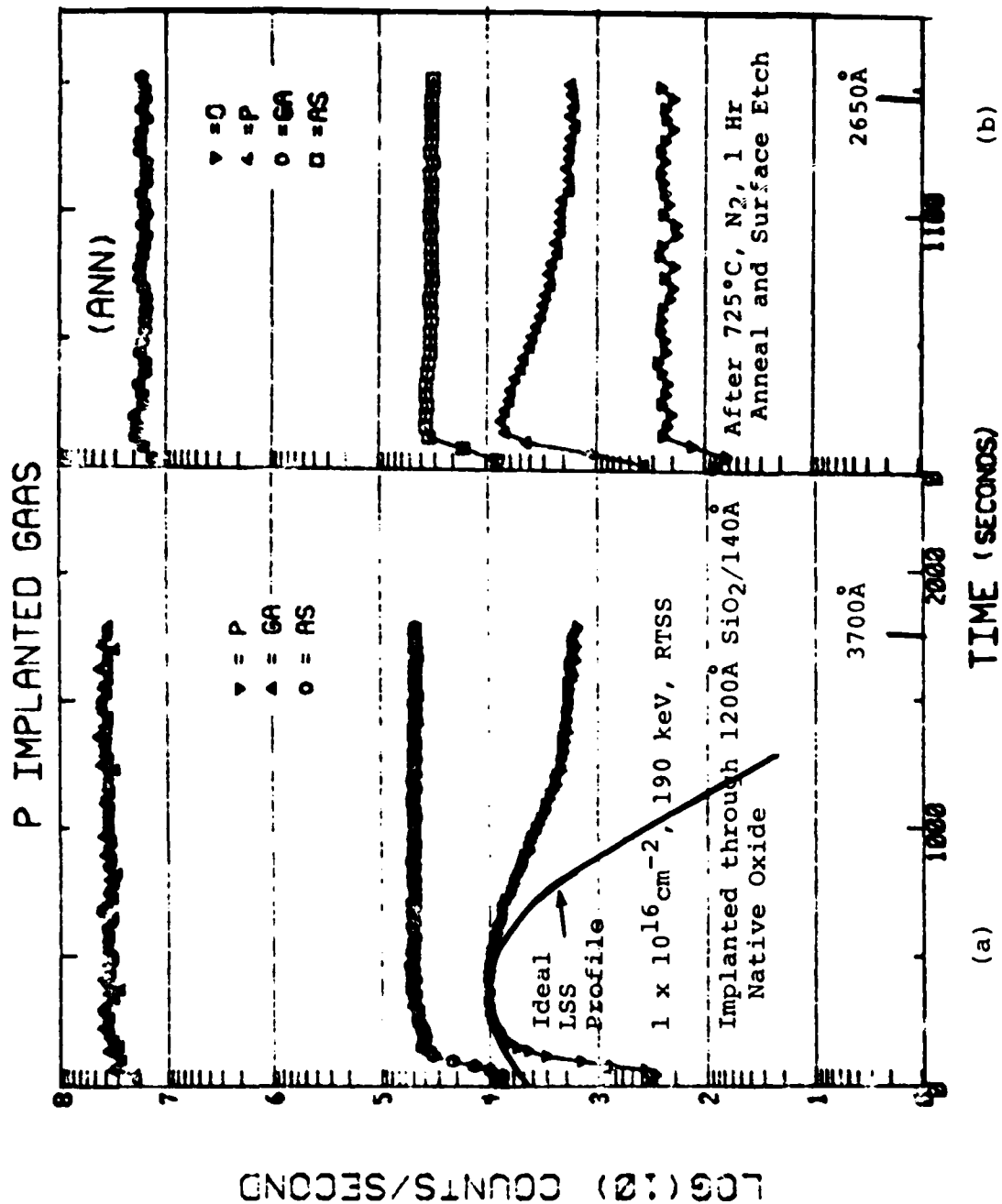


Figure 15. IMMA Profiles of Unannealed (a) and Annealed (b) Implanted Layers

Figure 16 shows the profile of a sample which was implanted to a dose of  $1 \times 10^{16} \text{ cm}^{-2}$  at 140 keV with a substrate temperature of 300°C. A strict comparison cannot be made between Figures 15 (a) and 16 because of the differing implant energies used; however, it appears that there is no significant phosphorus diffusion into the substrate as a result of the elevated temperature.

The elemental depth profile of an implanted and annealed sample, before and after oxidation at 600°C, is shown in Figures 17 (a) and (b). The oxide profile indicates that there is apparently incorporation of phosphorus into the oxide in the region from the peak of the implant to the interface of the semiconductor. There is a deficiency of arsenic in the outer region of the oxide layer, which has been observed before in oxides on both GaAs and  $\text{GaAs}_{1-x}\text{P}_x$ . However, due to the nature of the single implant used here, there is also a deficit of phosphorus at the oxide surface. Because of these facts, it appears that the surface region of the oxide may be primarily composed of gallium oxide ( $\text{Ga}_2\text{O}_3$ ).

The high surface concentration of oxygen in the annealed sample of Figure 17 (a) may be due either to an interaction of the gallium arsenide with the silicon dioxide cap at the annealing temperature of 725°C or to a residue of native oxide which was not removed by the HF strip prior to oxidation. Based upon previous etching studies of native oxides on  $\text{GaAs}_{1-x}\text{P}_x$  (References 2 and 3), the latter explanation is more likely.

Elemental profiles of oxides grown on unannealed surfaces generally show the same features as those on annealed surfaces. Figures 18 (a) - (c) show profiles of oxides grown on unimplanted GaAs and samples of differing phosphorus implant energies. Again, the surface region appears to be primarily  $\text{Ga}_2\text{O}_3$  due to the lack of arsenic and phosphorus.

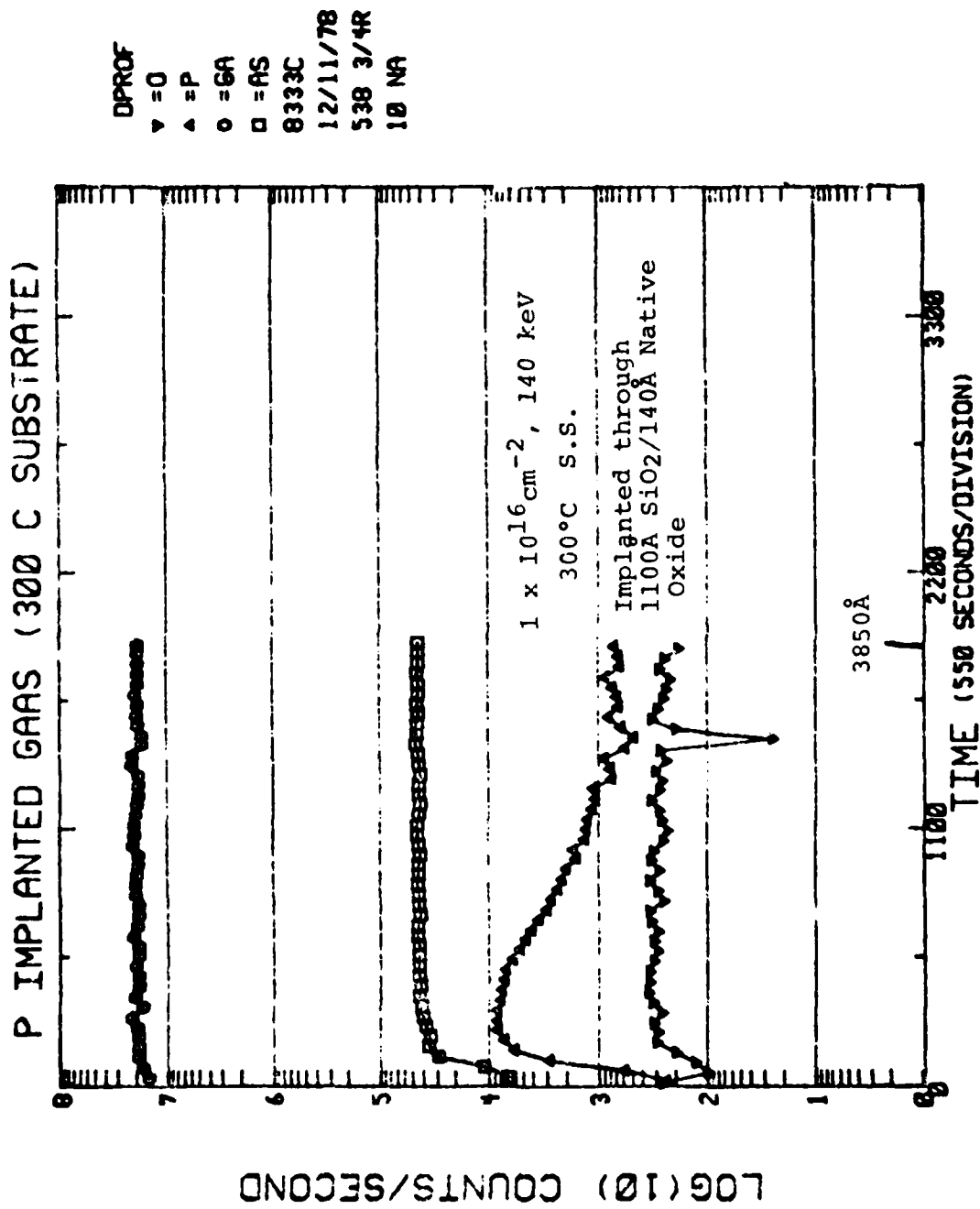


Figure 16. IMMA Profile of Sample Implanted at 300°C Substrate Temperature



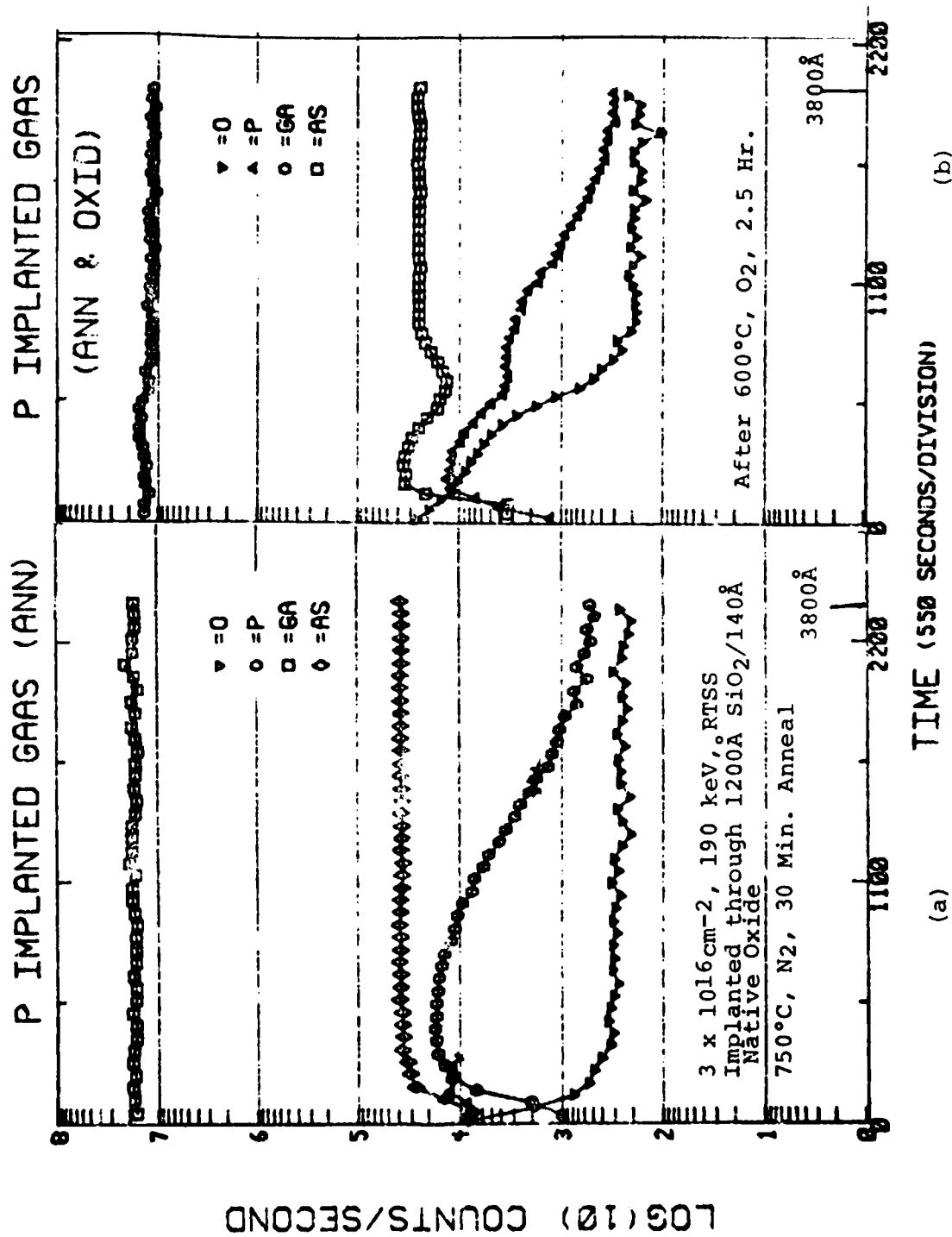


Figure 17. IMMA Profiles of Annealed (a) and Annealed/Oxidized (b) Implanted Layers

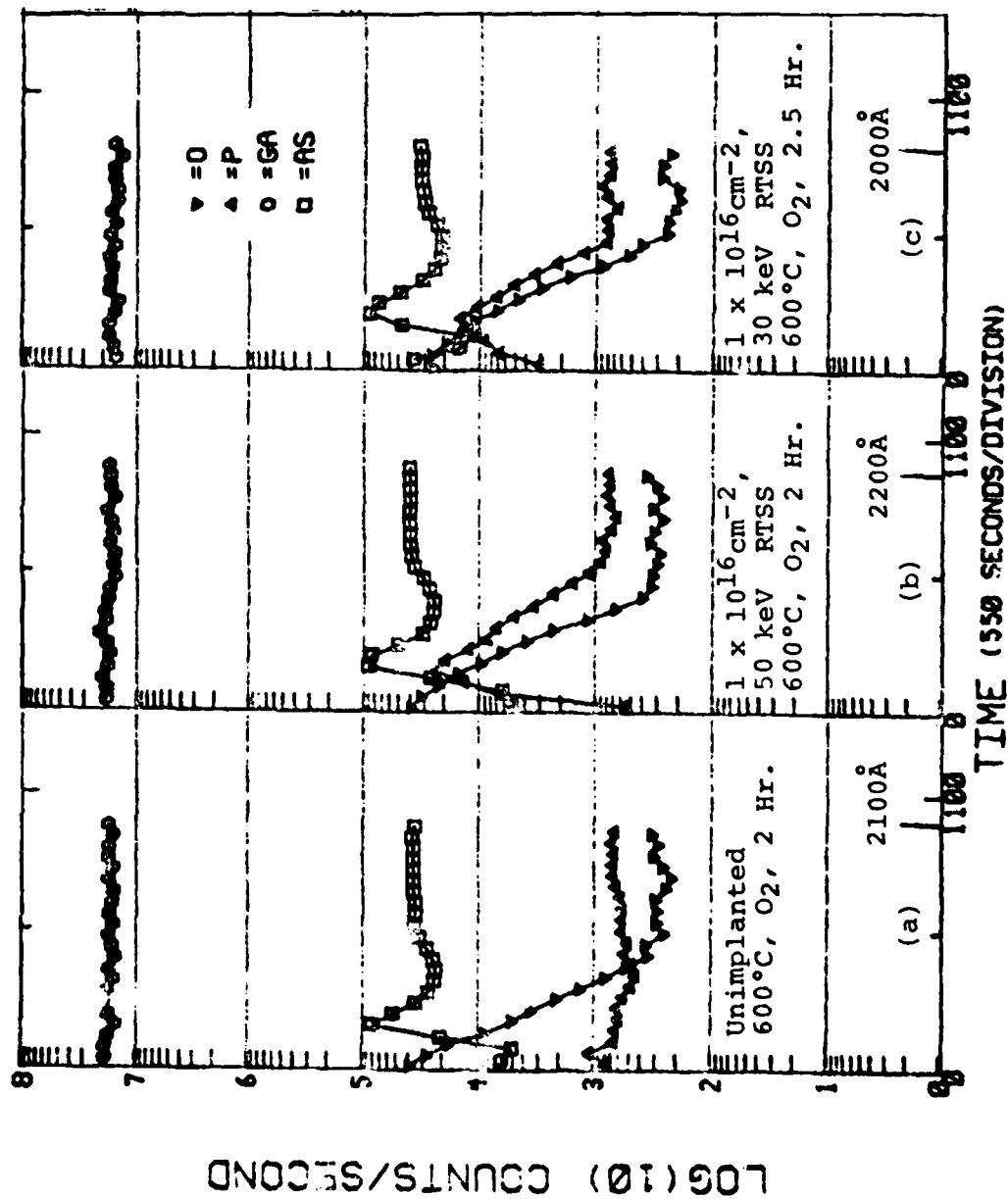


Figure 18. IMMA Profiles of Oxides Grown on Unimplanted(a) and Unannealed Implanted (b,c) Layers

## SECTION IV

### SUMMARY AND CONCLUSIONS

This section summarizes some of the major results obtained during the initial phase of this program and discusses areas where further investigations are needed.

#### Ion Implantation and Annealing

The ion implantation and encapsulation experiments conducted so far have indicated that silicon dioxide, deposited on a thin native oxide, provides the most effective encapsulant for high-temperature annealing of gallium arsenide surfaces implanted with a high dose of phosphorus ions. Annealing can be performed at temperatures up to 775°C using SiO<sub>2</sub> without decomposition of the semiconductor. However, further improvements in film quality are needed to achieve some of the higher annealing temperatures which have been reported in the literature.

The post-implant annealing experiments have demonstrated the ability of the high-dose phosphorus implant to significantly reduce decomposition under the encapsulant during high-temperature processing. This may have implications far beyond the immediate scope of this program.

The electron diffraction patterns indicate that the high-dose phosphorus implants do not result in massive lattice damage, although a more sensitive technique, such as ion backscattering, will be required to detect the defect levels which have been observed in earlier implants into GaAs.

Ion microprobe results indicate that there is no significant diffusion of phosphorus into the substrate during either post-implant annealing or hot substrate implantation. This indicates that the depth of the implanted region can be well controlled so that the advantageous properties of the underlying GaAs substrate can probably be utilized in subsequent MIS devices.

#### Oxidation

Oxides grown on the unannealed phosphorus-implanted surfaces have generally shown somewhat less decomposition and damage than those which were annealed with an encapsulant. The implant dose and energy variations attempted to date have narrowed the range of parameters for which acceptable oxides result. For unencapsulated surfaces it has been found that ions implanted at doses from  $1$  to  $2 \times 10^{16} \text{ cm}^{-2}$  and energies from  $30 \text{ keV}$  to  $60 \text{ keV}$  result in oxides with the fewest visible defects. Encouragingly, these oxides are visually similar to those grown on  $\text{GaAs}_{1-x}\text{P}_x$ , and suggest that further improvements could lead to similar electrical properties.

Oxides grown on both unannealed and annealed aluminum implanted surfaces show significant decomposition and gallium flow for conditions approximating those giving good results with phosphorus.

The C-V characteristics of oxides grown at  $600^\circ\text{C}$  in dry  $\text{O}_2$  over phosphorus implanted GaAs exhibit hysteresis and deep depletion somewhat similar to oxides grown on single-crystal  $\text{GaAs}_{1-x}\text{P}_x$ . D-c conductivity measurements indicate leakage current densities about an order of magnitude higher (for the same field) than those for oxides grown on  $\text{GaAs}_{1-x}\text{P}_x$ .

## CONCLUSIONS

The work to date has shown encouraging results relative to modifying the GaAs surface by implantation to permit uniform oxide growth. However, a device quality (electric) dielectric has not been achieved to date. A number of questions remain concerning the optimum dielectric growth procedure, as well as the impact of the implanted layer upon the insulator-semiconductor interface characteristics. Since many of these questions can only be answered by more in-depth analysis and experiments outside the scope of this program, work on this approach will conclude with this report.

## REFERENCES

1. D. H. Phillips, et al, J. Electrochem. Soc., 120, 1087 (1973)
2. R. K. Pancholy and D. H. Phillips, 19th Electronic Materials Conference, Cornell Univ., Ithaca, New York (1977)
3. G. J. Kuhlmann, et al, "GPO/GaAs<sub>0.5</sub>P<sub>0.5</sub> MOS Capacitors", Final Report, Contract DAAK70-77-C-0122, U. S. Army Night Vision Laboratory (Sept. 1977)
4. G. J. Kuhlmann, "A Study to Investigate the Chemical Stability of Gallium-Phosphate-Oxide/Gallium Arsenide Phosphide", Final Report, Contract NAS1-15101, NASA Langley Research Center (March 1978)
5. G. J. Kuhlmann, et al, Thin Solid Films (Jan. 1979)
6. R. P. H. Chang, et al, Appl. Phys. Lett., 30, 657, (1977)
7. R. P. H. Chang, et al, J. Appl. Phys., 48, 5384, (1977)
8. H. C. Casey, et al, Appl. Phys. Lett., 32, 678, (1978)
9. W. T. Tsang, Appl. Phys. Lett., 33, 426 (1978)
10. I. M. Belyi, et al, Sov. Phys Semicond., 9, 1326 (1976)
11. R. G. Hunsperger and O. J. Marsh, Appl. Phys. Lett., 19, 327 (1971)
12. G. A. Kachurin, et al, Sov. Phys. Semicond., 10, 919 (1976)
13. F. F. Kamarov and I. S. Tashlykov, Sov. Phys. Semicond., 11, 1156 (1977)
14. M. Rubenstein, J. Electrochem. Soc., 113, 540 (1966)
15. K. Loschke, et al, Thin Solid Films, 48, 229 (1978)
16. J. J. Tietjen and L. R. Weisberg, Appl. Phys. Lett., 7, 10 (1965)
17. J. F. Gibbons, et al, Projected Range Statistics, 2nd Edition, Dowden, Hutchinson, Inc., Stroudsburg, Pa., (1975)
18. S. M. Sze, Physics of Semiconductor Devices, John Wiley and Sons New York, NY (1969)
19. O. N. Kuznetsov, et al, Sov. Phys. Semicond., 11, 851 (1977)
20. K. V. Vaidyanathan, et al, J. Electrochem. Soc., 124, 1781 (1977)
21. T. Inada, et al, J. Appl. Phys., 49, 4571 (1978)

22. E. C. Bell, et al, Thin Solid Films, 51, 77 (1978)
23. I. Ohdomari, et al, Appl. Phys. Lett., 32, 218 (1978)
24. B. Molnar, J. Electrochem. Soc., 123, 767, (1976)
25. C. L. Ramiller, et al, "Comparison of Pyrolytic and Plasma-Deposited SiO<sub>2</sub>, Si<sub>3</sub>N<sub>4</sub> and SiO<sub>x</sub>N<sub>y</sub> as Encapsulants for Se-Implanted GaAs", Electrochemical Society Meeting, Seattle, Wash., May 1978
26. A. Lidow, et al, J. Appl. Phys., 49, 5213 (1978)
27. A. A. Immorlica and F. H. Eisen, Appl. Phys. Lett., 29, 94 (1976)
28. R. M. Malbon, et al, J. Electrochem. Soc., 123, 1413 (1976)
29. R. P. Mandal and W. R. Scoble, 7th International Symposium on GaAs and Related Compounds, St. Louis, Mo., Sept. 1978
30. G. J. Kuhlmann, unpublished data, 1978
31. G. C. Jain, et al, Solid State Electron., 19, 731 (1976)
32. R. Zuleeg, et al, "Enhancement Mode GaAs JFET Medium-Scale Integrated Circuit Technology", Interim Technical Report. Contract F33615-76-C-1127, Air Force Avionics Laboratory, Sept. 1977
33. I. Shiota, et al, J. Electrochem. Soc., 124, 1405 (1977)
34. W. J. Anderson and Y. S. Park, J. Appl. Phys., 46, 4563 (1978)
35. J. W. Werner, Acta Electronica, 19, 53 (1976)

DATE

FILMED

-8